



Canadian Journal of Physiology and Pharmacology

Muscarinic agonists inhibit the ATP-dependent potassium current and suppress the ventricle-Purkinje action potential dispersion

Journal:	<i>Canadian Journal of Physiology and Pharmacology</i>
Manuscript ID	cjpp-2020-0408.R1
Manuscript Type:	Article
Date Submitted by the Author:	01-Nov-2020
Complete List of Authors:	Magyar, Tibor; University Szeged, Department of Pharmacology and Pharmacotherapy Árpádfy-Lovas, Tamás; University of Szeged, Pharmacology and Pharmacotherapy Pászti, Bence; University Szeged, Department of Pharmacology and Pharmacotherapy Tóth, Noémi; Szegedi Tudományegyetem, Department of Pharmacology and Pharmacotherapy Gyökeres, András; Szegedi Tudományegyetem, Department of Pharmacology and Pharmacotherapy Györe, Balázs; University of Szeged Gurabi, Zsolt ; Szegedi Tudományegyetem, Department of Pharmacology and Pharmacotherapy Nagy, Norbert; University of Szeged, MTA-SZTE Research Group of Cardiovascular Pharmacology, Hungarian Academy of Sciences Jost, Norbert; HUngarian Academy of Sciences, Division of Cardiovascular Pharmacology Virág, László; University of Szeged, Department of Pharmacology and Pharmacotherapy; HUngarian Academy of Sciences, Division of Cardiovascular Pharmacology Papp, Julius; University of Szeged,, Department of Pharmacology and Pharmacotherapy Koncz, Istvan; Szegedi Tudományegyetem, Department of Pharmacology and Pharmacotherapy
Is the invited manuscript for consideration in a Special Issue:	Joint North American/European IACS 2019
Keyword:	acetylcholine, Purkinje fibers, papillary muscles, hypoxia

SCHOLARONE™
Manuscripts

**Muscarinic agonists inhibit the ATP-dependent potassium current and suppress the
ventricle-Purkinje action potential dispersion**

Tibor Magyar^{a,§}, Tamás Árpádfy-Lovas^{a,§}, Bence Pásztai^a, Noémi Tóth^a, Jozefína Szlovák^a,
Péter Gazdag^a, Zsófia Kohajda^b, András Gyökeres^a, Balázs Györe^d, Zsolt Gurabi^a, Norbert
Jost^{a,b,c}, László Virág^{a,c}, Julius Gy. Papp^{a,b}, Norbert Nagy^{a,b,#}, István Koncz^{a,*,#}

^aDepartment of Pharmacology and Pharmacotherapy, Faculty of Medicine, University of
Szeged, Szeged, Hungary;

^bMTA-SZTE Research Group of Cardiovascular Pharmacology, Hungarian Academy of
Sciences, Szeged, Hungary

^cDepartment of Pharmacology and Pharmacotherapy, Interdisciplinary Excellence Centre,
University of Szeged, Szeged, Hungary

^dFaculty of Dentistry, University of Szeged, Hungary

§ Shared first authorship

Shared senior authorship

*Author for correspondence at:

István Koncz MD, PhD

Department of Pharmacology & Pharmacotherapy

Faculty of Medicine

University of Szeged

Dóm tér 12,

H-6720 Szeged, Hungary

E-mail: koncz.istvan@med.u-szeged.hu

28 **Abstract**

29 **Introduction:** Activation of the parasympathetic nervous system has been reported to have an
30 antiarrhythmic role during ischemia-reperfusion injury by decreasing the arrhythmia triggers.
31 Furthermore, it was reported that the parasympathetic neurotransmitter acetylcholine is able to
32 modulate the ATP-dependent K-current (I_{K-ATP}), a crucial current activated during hypoxia.
33 However, the possible significance of this current modulation in the antiarrhythmic
34 mechanism is not fully clarified.

35 **Methods:** Action potentials were measured using the conventional microelectrode technique
36 from canine left ventricular papillary muscle and free-running Purkinje fibers, under normal
37 and hypoxic conditions. Ionic currents were measured using the whole-cell configuration of
38 the patch clamp method.

39 **Results:** 5 μ M acetylcholine did not influence the action potential duration (APD) either in
40 Purkinje fibers or in papillary muscle preparations. In contrast, it significantly lengthened the
41 APD and suppressed the Purkinje–ventricle APD dispersion when it was administered after
42 5 μ M pinacidil application. 3 μ M carbachol reduced the pinacidil-activated I_{K-ATP} under
43 voltage-clamp condition. Acetylcholine lengthened the ventricular action potential under
44 simulated ischemia condition.

45 **Conclusion:** In this study we found that acetylcholine inhibits the I_{K-ATP} and thus suppresses
46 the ventricle-Purkinje APD dispersion. We conclude that parasympathetic tone may reduce
47 the arrhythmogenic substrate exerting a complex antiarrhythmic mechanism during hypoxic
48 conditions.

49

50 *Key words:* acetylcholine, Purkinje fibers, papillary muscles, hypoxia

Introduction

The parasympathetic nervous system has a crucial role in controlling the actual heart rate and impulse propagation via influencing the sinoatrial and atrioventricular nodes (Higgins et al., 1973). The parasympathetic nerve endings operate by releasing acetylcholine that acts on M_2 -receptors, activating several intracellular signaling routes, and ultimately influencing the cardiac ion channels (Harvey and Belevych, 2003). Even though the parasympathetic nervous system primarily innervates the supraventricular areas of the heart, there are certain important ion channels in the ventricular muscle that are known to be influenced by the release of acetylcholine. It has been previously reported that the inward rectifier potassium current (I_{K1} ; Koumi et al., 1995) and the slow component of the delayed rectifier (I_{Ks} ; Pappano and Carmeliet, 1979) are inhibited, whereas I_{K-ATP} and I_{K-ACh} are activated by acetylcholine via G proteins (Terzic et al., 1994; Ito et al., 1994; Kim et al., 1997).

The importance of these effects of acetylcholine is underpinned by the fact that the activation of I_{K-ATP} channels is well known during hypoxia/ischemia, in which situations the duration of the action potential is shortened (Weiss and Venkatesh, 1993). Furthermore, it was reported that vagal activation is also facilitated under ischemia–reperfusion (Recordati et al., 1971). This vagal activation during hypoxia could be antiarrhythmic, since it was reported that increased parasympathetic tone reduces the catecholaminergic-induced early and delayed afterdepolarizations (arrhythmia triggers) (Song et al., 1992), as well as the incidence of ventricular fibrillation (Zuanetti et al., 1987; Collins and Billman, 1989). However, the underlying mechanism of antiarrhythmic effect of M_2 -receptor activation is not fully clarified. Arrhythmias may develop when an arrhythmogenic substrate (e. g., dispersion of repolarization) and arrhythmia triggers (e.g.: early and delayed afterdepolarizations) simultaneously exist in the heart. The arrhythmogenic substrate could be prominent at Purkinje–ventricle connection because of the relatively weak electrotonic coupling due to low number of gap junctions (Varró and Baczkó, 2010). As a consequence of the different

pharmacological susceptibility of Purkinje fiber and ventricular muscle (Baláti et al, 1998), the activation of I_{K-ATP} may modulate the Purkinje and ventricular action potential duration (APD) to different extents, and the developed APD dispersion may contribute to the onset of arrhythmias.

The objective of this study was the investigation of the possible effect of acetylcholine on the I_{K-ATP} and on the I_{K-ATP} -mediated action potential dispersion under normal and hypoxic conditions.

Methods

Human tissues

Non-diseased human hearts that were unusable for transplantation (based on logistical, not patient-related considerations) were obtained from organ donors. Before cardiac explantation, organ donor patients did not receive medication except dobutamine, furosemide and plasma expanders. The investigations conform to the principles outlined in the *Declaration of Helsinki* of the World Medical Association. All experimental protocols were approved by the Scientific and Research Ethical Committee of the Medical Scientific Board at the Hungarian Ministry of Health (ETT-TUKEB), under ethical approval No 4991-0/2010-1018EKU (339/PI/010). Human cardiac tissue was stored in cardioplegic solution at 4°C for 4–8 hours.

Animals

All experiments using canine cardiac preparations were carried out in compliance with the Guide for the Care and Use of Laboratory Animals (USA NIH publication NO 85-23, revised 1996) and conformed to the Directive 2010/63/EU of the European Parliament. The protocols have been approved by the Ethical Committee for the Protection of Animals in Research of the University of Szeged, Szeged, Hungary (approval number: I-74-24-2017) and by the

Department of Animal Health and Food Control of the Ministry of Agriculture and Rural Development (authority approval number XIII/3331/2017).

Conventional microelectrode technique

Ventricular (papillary or trabecular) muscles were obtained from the right ventricle of canine hearts. Free-running Purkinje fibers were identified as false tendons and isolated from both ventricles of human and canine hearts. Canine hearts were removed through a right lateral thoracotomy from anesthetized (thiopental 30 mg/kg i.v.) mongrel dogs of either sex weighing 10–15 kg. At impalement, Purkinje fibers were observed under a surgical microscope (Zeiss OPMI PRO). The preparations were placed in Locke's solution and allowed to equilibrate for at least 2 hours while superfused (flow rate 4-5 ml/min) also with Locke's solution containing (in mM): NaCl 120, KCl 4, CaCl₂ 2, MgCl₂ 1, NaHCO₃ 22, and glucose 11. The pH of this solution was 7.40 to 7.45 when gassed with 95% O₂ and 5% CO₂ at 37 °C. In the experiments where the effects of tissue hypoxia were examined, we changed the gas mixture to 95% N₂ and 5% CO₂, pH remained at 7.40 to 7.45. All experiments were performed at 37 °C. During the equilibration period, preparations were stimulated at a basic cycle length of 500 ms. Electrical pulses of 0.5–2 ms in duration at twice the diastolic threshold in intensity (S₁) were delivered to the preparations through bipolar platinum electrodes. Transmembrane potentials were recorded using glass capillary microelectrodes filled with 3 M KCl (tip resistance: 5 to 15 MΩ). The microelectrodes were coupled through an Ag-AgCl junction to the input of a high-impedance, capacitance-neutralizing amplifier (Experimetria 2011). Intracellular recordings were displayed on a storage oscilloscope (Hitachi V-555) and led to a computer system (APES) designed for on-line determination of the following parameters: resting membrane potential, action potential amplitude, action potential duration at 10% to 90% repolarization and the maximum rate of rise of the action potential upstroke (V_{max}). Control recordings were obtained after equilibration period. The compounds used in all experiments were purchased from Sigma/Merck.

2.3. Cell isolation

Ventricular myocytes were enzymatically dissociated from the left ventricle of dog hearts. Canine hearts were removed through a right lateral thoracotomy from anesthetized (thiopental 30 mg/kg i.v.) mongrel dogs of either sex weighing 10–15 kg. Cardiac myocytes were isolated from the left ventricle, containing an arterial branch through which the segment was perfused on a Langendorff apparatus with solutions in the following sequence: normal Tyrode's solution (containing in mM: 144 mM NaCl, 0.4 mM NaH₂PO₄, 4 mM KCl, 0.53 mM MgSO₄, 1.8 mM CaCl₂, 5.5 mM Glucose, 5 mM HEPES, pH 7.4 adjusted with NaOH) for 10 min, Ca²⁺-free Tyrode solution for 10 min and Ca²⁺-free Tyrode solution containing collagenase (Worthington type II, 0.66 mg/mL). To the final perfusion solution protease (type XIV, 0.12 mg/mL) was added at the 15 and the 30 minutes for digestion.

2.4. Measurement of ionic currents

One drop of cell suspension was placed in a transparent recording chamber mounted on the stage of an inverted microscope (Olympus IX51, Tokyo, Japan), and individual myocytes were allowed to settle and adhere to the chamber bottom for at least 5–10 min before superfusion was initiated and maintained by gravity. Only rod-shaped cells with clear striations were used. HEPES-buffered Tyrode's solution (composition in mM: NaCl 144, NaH₂PO₄ 0.4, KCl 4.0, CaCl₂ 1.8, MgSO₄ 0.53, glucose 5.5 and HEPES 5.0, at pH of 7.4) was used as the normal superfusate. During the measurement of I_{K-ATP} , 1 μ M nisoldipine was added to the bath solution to block I_{CaL} , I_{Kr} was blocked by 0.1 μ M dofetilide, and I_{Ks} was blocked by 0.5 μ M HMR-1556. Micropipettes were fabricated from borosilicate glass capillaries (Science Products GmbH, Hofheim, Germany), using a P-97 Flaming/Brown micropipette puller (Sutter Co, Novato, CA, USA), and had a resistance of 1.5–2.5 M Ω when filled with pipette solution. The membrane currents were recorded with Axopatch-200B amplifiers (Molecular Devices, Sunnyvale, CA, USA) by applying the whole-cell configuration of the patch-clamp technique. The membrane currents were digitized with 250

kHz analogue to digital converters (Digidata 1440A, Molecular Devices, Sunnyvale, CA, USA) under software control (pClamp 8 and pClamp 10, Molecular Devices, Sunnyvale, CA, USA). The composition of the pipette solution (in mM) was the following: KOH 110, KCl 40, K₂ATP 5, MgCl₂ 5, EGTA 5, HEPES 10 and GTP 0.1 (pH was adjusted to 7.2 by aspartic acid).

2.5 Statistical analysis

Results are expressed as mean \pm S.E.M. Normality of distributions was verified using Shapiro-Wilk test, and homogeneity of variances was verified using Bartlett's test in each treatment group. Statistical comparisons were made using analysis of variance (ANOVA) for repeated measurements, followed by Bonferroni's post-hoc test. Differences were considered significant when $p < 0.05$.

Results

1. Acetylcholine lengthened the APD after pinacidil-mediated action potential shortening

Canine Purkinje fibers and ventricular papillary muscles were paced at 500 ms cycle length. In canine Purkinje fibers (PFs; n=15), acetylcholine (5 μ M) did not affect the repolarization (233.6 \pm 4.7 to 231.7 \pm 4.6; Figures 1A and 1E). In contrast, in canine Purkinje fibers (n=8), the I_{K-ATP} activator pinacidil, applied in 5 μ M concentration, significantly abbreviated APD₉₀ (207.7 \pm 7.0 ms vs 113.1 \pm 9.1 ms, $p < 0.05$) values. After steady state was reached, acetylcholine was administered. Within 3 minutes, acetylcholine prolonged APD₉₀ to 147.3 \pm 7.4 ms, partially reversing the effects of pinacidil (Figures 1B and 1E; $p < 0.05$).

Similarly, as observed in Purkinje fibers, 5 μ M acetylcholine alone failed to influence the APD of the ventricular muscle (APD₉₀: 172.6 \pm 5.7 ms vs 172.8 \pm 5.3 ms). Pinacidil (n=5; 5 μ M) pretreatment significantly abbreviated the APD₉₀ value (187.9 \pm 4.5 ms vs 163.7 \pm 6.4 ms, $p < 0.05$), similarly to the effects observed in the case of PFs. After a period of

30 minutes, sufficient to reach a steady state, acetylcholine was added to the superfusate. Within 4 minutes, acetylcholine (5 μ M) prolonged APD₉₀ to 172.1 \pm 7.4 ms ($p<0.05$), thus partially reversing the effects of pinacidil (Figures 1D and 1E).

2. Acetylcholine decreased the calculated APD dispersion between PF and VM

The changes in the difference between the APD₉₀ values of PF and VM can be used to infer the effects of pinacidil and acetylcholine on the dispersion between these cardiac tissue types (Figure 2). The control APD₉₀ dispersion (9.5%, 20 ms) was significantly increased upon 5 μ M pinacidil application (44.7%, 51 ms). On the other hand, subsequently applied 5 μ M acetylcholine markedly decreased the repolarization heterogeneity (16.9%, 28 ms; $p<0.05$).

3. Carbachol decreased the pinacidil-induced current activation

During ionic current measurements, voltage ramps were used from a holding potential of -90 mV. Membrane potential was hyperpolarized to -120 mV, and then was slowly (over 36 s) depolarized to 60 mV. Ionic currents were analyzed and compared at 0 and +30 mV. We found that carbachol did not change the control current when it was applied *without* pinacidil (0 mV - control: 0.20 \pm 0.2 pA/pF vs 3 μ M carbachol: 0.32 \pm 0.2 pA/pF, $n=6$ and +30 mV - control: 0.55 \pm 0.4 pA/pF vs 3 μ M carbachol: 0.74 \pm 0.3 pA/pF, $n=6$). In contrast, when 5 μ M pinacidil was applied first, subsequently employed carbachol significantly reduced the current at both voltages (0 mV – control: 0.24 \pm 0.2 pA/pF \rightarrow 5 μ M pinacidil: 2.03 \pm 0.3 pA/pF \rightarrow 3 μ M carbachol: 1.51 \pm 0.4 pA/pF, $n=8$, $p<0.05$. +30 mV - control: 0.78 \pm 0.6 pA/pF \rightarrow 5 μ M pinacidil: 3.17 \pm 0.3 pA/pF \rightarrow 3 μ M carbachol: 2.26 \pm 0.3 pA/pF, $n=8$, $p<0.05$).

These measurements were carried out with acetylcholine as well. However, we found carbachol to be more stable during the applied long voltage protocol.

4. Acetylcholine restored the APD after hypoxia-induced action potential shortening

Simulated hypoxia, achieved by gassing the solution with N₂ and CO₂ instead of O₂ and CO₂, resulted in a significant abbreviation of APD₉₀ from 181.4±5.7 ms to 135.0±8.6 ms ($p<0.05$, Figures 4A and 4B), and a decrease in amplitude (103.7±2.8 mV vs 92±3.5 mV). The maximum rate of depolarization was also decreased (185.8±15.8 V/s vs 156.1±20.6 V/s). When applied during hypoxia, 5 µM acetylcholine caused a significant APD₉₀ prolongation to 164.4±4.4 ms, partially reversing the effect of hypoxia on the repolarization. AMP returned to a normal range (102.1±1.6 mV), while V_{max} remained at 156.0±16.1 V/s.

5. Acetylcholine caused a slight abbreviation in human Purkinje fibers

In human PFs (n=2), acetylcholine in 5 µM concentration caused a slight abbreviation of APD₉₀ from 269.0±28.4 to 251.6±42.85 ms and APD₅₀ from 184.4±20.0 ms to 173.3±27.1 ms without affecting other characteristics of the action potential (Figure 5).

Discussion

In this study we investigated the electrophysiological effects of muscarinic agonists on the I_{K-ATP} current. We found that (i) under normal conditions acetylcholine did not influence the action potential duration. (ii) In contrast, when I_{K-ATP} was pharmacologically activated by pinacidil, subsequently applied acetylcholine lengthened the action potential duration as well as (iii) reduced the pinacidil-induced ventricle-Purkinje APD dispersion. (iv) In line with this, carbachol inhibited the I_{K-ATP} that was previously activated by pinacidil. (v) Acetylcholine increased the APD after hypoxia-induced action potential shortening.

Acetylcholine inhibits the I_{K-ATP} in canine ventricular myocytes

It is well known that acetylcholine shortens the atrial APD and has been implicated in atrial fibrillation (Nakayama et al, 1968). Acetylcholine directly affects the GIRK1/4 or Kir3.1/Kir3.4 channels (Nobles et al, 2018; Corey and Clapham, 1998), encoded by *KCNJ3*

and *KCNJ4* genes (Kurachi, 1995). These channels are largely expressed in atrial, SA and AV nodal cells (Galindo et al, 2016; Navarro-Polanco et al, 2013). At the same time, previous studies (Terzic et al, 1994; Ito et al., 1994) claimed that acetylcholine activates the I_{K-ATP} channels, even though the physiological consequences of this effect on the action potential were not clarified.

The I_{K-ATP} ATP-sensitive potassium channels comprise hetero-octamers consisting of four inward rectifying potassium channel pore-forming subunits (Kir6.1 or Kir6.2, encoded by *KCNJ8* and *KCNJ11* genes, respectively) and four ATP-binding cassette protein sulphonylurea receptors (SUR1 or SUR2, encoded by *ABCC8* and *ABCC9* genes, respectively; Inagaki et al, 1995). An important feature of the I_{K-ATP} is its closed state under physiological intracellular ATP levels (i. e., under normoxia) and its activation by metabolic stress, when the ratio of ATP/ADP is decreased, e. g., during myocardial ischemia (Deutsch et al., 1991).

Activation of the sarcolemmal I_{K-ATP} during myocardial ischemia shortens the action potential of various cardiac tissues to different extents, thus it may promote APD dispersion and re-entry type arrhythmias (Janse and Wit, 1989). Accordingly, several investigations found I_{K-ATP} activation to be pro-arrhythmic (Chi et al., 1990), suggesting that sarcolemmal I_{K-ATP} inhibition may prevent arrhythmias induced by myocardial ischemia and ischemia/reperfusion (Billman et al, 1998; Englert et al, 2003; Vajda et al, 2007).

In our experiments under normal conditions, we found no effect of carbachol on the membrane current (Figure 3) and, similarly, acetylcholine failed to influence the ventricular and Purkinje APDs (Figures 1A and 1C). The observed discrepancy between our and previous results, where an activation of I_{K-ATP} was described upon acetylcholine administration (Terzic

et al, 1994; Ito et al, 1994; Kim et al., 1997), could be the consequence of the species difference and the distinct experimental conditions.

In contrast, an important, and, to the best of our knowledge, previously not published result of our study is that carbachol is able to suppress the pinacidil-activated I_{K-ATP} . As a consequence, in parallel tissue action potential experiments, acetylcholine lengthened the APD as long as it was previously shortened by the application of I_{K-ATP} -activator pinacidil. Since I_{K-ATP} activation could be arrhythmogenic (Chi et al., 1990) by causing an increase in the APD dispersion, this effect of acetylcholine raises the possibility of a novel antiarrhythmic mechanism of the previously described antiarrhythmic effect of parasympathetic activation during hypoxia (Song et al., 1992; Zuanetti et al., 1987; Collins and Billman, 1989).

Our experiments conducted under hypoxic conditions provided similar results (i. e., acetylcholine lengthened the hypoxia-induced shortened ventricular action potential; Figure 4). Even though tissue hypoxia is a complex phenomenon (Carmeliet, 1999), during which several factors change simultaneously (e. g., Ca^{2+}_i , Na^+_i , pH, conductance of gap junctions, membrane potential etc.), it is feasible that I_{K-ATP} activation, as a response to ATP depletion, is an important factor in the observed action potential shortening. Since acetylcholine lengthened the action potential under hypoxic conditions, we suggest I_{K-ATP} inhibition as a possible underlying mechanism.

Acetylcholine decreased the pinacidil-induced ventricle–Purkinje APD dispersion

Free-running Purkinje fibers connect to the ventricular muscle on a small surface area, providing a relatively large-resistance coupling (Tranum-Jensen et al., 1991), and a large sink for current flow that favors conduction blocks more than other parts of the healthy myocardium. Also, due to the weaker electrotonic coupling, the dispersion of repolarization here can be greater than in other areas (Martinez et al., 2018), causing the Purkinje–ventricle

APD ratio to have critical importance in arrhythmia generation. In our experiments, we found significantly greater shortening in Purkinje fibers caused by pinacidil that could be the consequence of the generally weaker repolarization reserve that makes the Purkinje action potential to be more susceptible to any pharmacological interventions (Varró et al, 2000; Baláti et al, 1998). Similarly, acetylcholine exerted larger lengthening in the Purkinje fiber probably by the same reason that ultimately led to reduced ventricle–Purkinje APD dispersion. The reduction of the ventricle–Purkinje fiber APD dispersion could suppress the arrhythmogenic substrate providing a narrower vulnerable period for a critically timed extrasystole to trigger a life-threatening arrhythmia under hypoxic conditions.

Proposed mechanism

Since inhibition of the I_{K-ATP} channels is possible by blocking various PKA-mediated pathways (Tinker et al, 2018.), we suggest that the decrease of cAMP levels caused by the activation of cardiac muscarinic receptors using acetylcholine/carbachol was the factor that decreased the density of the I_{K-ATP} current in patch clamp measurements, leading to the subsequent prolongation observed in action potential durations.

Conclusions

We found that muscarinic agonists inhibit the I_{K-ATP} . Therefore, during I_{K-ATP} -mediated action potential shortening, acetylcholine causes asymmetrical action potential lengthening between ventricular muscle and Purkinje fiber that leads to reduced APD dispersion.

These results suggest that the parasympathetic tone beyond suppressing the catecholaminerg-induced arrhythmogenic triggers (Song et al., 1992) may be also able to reduce the arrhythmogenic substrate under hypoxic conditions.

Study Limitations

(i) In our experiments, the ventricular and Purkinje fiber action potentials were measured from electrically uncoupled tissue samples.

(ii) The presented effects were attributed to the M2 muscarinic receptor; nevertheless, the exact level of contribution of other receptor subtypes was not addressed. To achieve this, further studies are needed, utilizing specific agonist and antagonist drugs.

Acknowledgments

We are grateful to Dr. Károly Acsai for his valuable contribution in performing statistical comparisons. This work was supported by grants from the National Research, Development and Innovation Office – NKFIH PD-116011 (for IK), FK-129117 (for NN) and the ÚNKP-18-4, 19-4 and ÚNKP-20-5-SZTE-165 New National Excellence Program of the Ministry for Innovation and Technology (for IK and NN), the János Bolyai Research Scholarship of the Hungarian Academy of Sciences (for NN) and EFOP-3.6.2-16-2017-00006 (LIVE LONGER) and EFOP 3.6.3-VEKOP-16-2017-00009 and Ministry of Human Capacities, Hungary grant 20391-3/2018/FEKUSTRAT, and the University of Szeged.

References

- Baláti, B., Varró, A., & Papp, J. G. (1998). Comparison of the cellular electrophysiological characteristics of canine left ventricular epicardium, M cells, endocardium and Purkinje fibers. *Acta Physiologica Scandinavica*, 164(2), 181–190. <https://doi.org/10.1046/j.1365-201X.1998.00416.x>
- Billman, G. E., Englert, H. C., & Schölkens, B. A. (1998). HMR 1883, a novel cardioselective inhibitor of the ATP-sensitive potassium channel. Part II: Effects on susceptibility to ventricular fibrillation induced by myocardial ischemia in conscious dogs. *The Journal of Pharmacology and Experimental Therapeutics*, 286(3), 1465–1473.
- Carmeliet, E. (1999). Cardiac ionic currents and acute ischemia: From channels to arrhythmias. *Physiological Reviews*, 79(3), 917–1017. <https://doi.org/10.1152/physrev.1999.79.3.917>
- Chi, L., Uprichard, A. C., & Lucchesi, B. R. (1990). Profibrillatory actions of pinacidil in a conscious canine model of sudden coronary death. *Journal of Cardiovascular Pharmacology*, 15(3), 452–464. <https://doi.org/10.1097/00005344-199003000-00016>
- Collins, M. N., & Billman, G. E. (1989). Autonomic response to coronary occlusion in animals susceptible to ventricular fibrillation. *The American Journal of Physiology*, 257(6 Pt 2), H1886–1894. <https://doi.org/10.1152/ajpheart.1989.257.6.H1886>
- Corey, S., & Clapham, D. E. (1998). Identification of native atrial G-protein-regulated inwardly rectifying K⁺ (GIRK4) channel homomultimers. *The Journal of Biological Chemistry*, 273(42), 27499–27504. <https://doi.org/10.1074/jbc.273.42.27499>
- Deutsch, N., Klitzner, T. S., Lamp, S. T., & Weiss, J. N. (1991). Activation of cardiac ATP-sensitive K⁺ current during hypoxia: Correlation with tissue ATP levels. *The American Journal of Physiology*, 261(3 Pt 2), H671–676. <https://doi.org/10.1152/ajpheart.1991.261.3.H671>
- Englert, H. C., Heitsch, H., Gerlach, U., & Knieps, S. (2003). Blockers of the ATP-sensitive potassium channel SUR2A/Kir6.2: A new approach to prevent sudden cardiac death. *Current Medicinal Chemistry. Cardiovascular and Hematological Agents*, 1(3), 253–271. <https://doi.org/10.2174/1568016033477423>

366

367 Harvey, R. D., & Belevych, A. E. (2003). Muscarinic regulation of cardiac ion channels. *British Journal of*
368 *Pharmacology*, 139(6), 1074–1084. <https://doi.org/10.1038/sj.bjp.0705338>

369

370 Higgins, C. B., Vatner, S. F., & Braunwald, E. (1973). Parasympathetic control of the heart. *Pharmacological*
371 *Reviews*, 25(1), 119–155.

372

373 Inagaki, N., Gono, T., Clement, J. P., Namba, N., Inazawa, J., Gonzalez, G., Aguilar-Bryan, L., Seino, S., &
374 Bryan, J. (1995). Reconstitution of IKATP: An inward rectifier subunit plus the sulfonylurea receptor. *Science*
375 *(New York, N.Y.)*, 270(5239), 1166–1170. <https://doi.org/10.1126/science.270.5239.1166>

376

377 Ito, H., Vereecke, J., & Carmeliet, E. (1994). Mode of regulation by G protein of the ATP-sensitive K⁺ channel
378 in guinea-pig ventricular cell membrane. *The Journal of Physiology*, 478 (Pt 1), 101–107.

379 <https://doi.org/10.1113/jphysiol.1994.sp020233>

380

381 Janse, M. J., & Wit, A. L. (1989). Electrophysiological mechanisms of ventricular arrhythmias resulting from
382 myocardial ischemia and infarction. *Physiological Reviews*, 69(4), 1049–1169.

383 <https://doi.org/10.1152/physrev.1989.69.4.1049>

384

385 Kim, D., Watson, M., & Indyk, V. (1997). ATP-dependent regulation of a G protein-coupled K⁺ channel
386 (GIRK1/GIRK4) expressed in oocytes. *The American Journal of Physiology*, 272(1 Pt 2), H195–206.

387 <https://doi.org/10.1152/ajpheart.1997.272.1.H195>

388

389 Koumi, S., Wasserstrom, J. A., & Ten Eick, R. E. (1995). Beta-adrenergic and cholinergic modulation of the
390 inwardly rectifying K⁺ current in guinea-pig ventricular myocytes. *The Journal of Physiology*, 486 (Pt 3), 647–

391 659. <https://doi.org/10.1113/jphysiol.1995.sp020841>

392

393 Kurachi, Y. (1995). G protein regulation of cardiac muscarinic potassium channel. *The American Journal of*
394 *Physiology*, 269(4 Pt 1), C821–830. <https://doi.org/10.1152/ajpcell.1995.269.4.C821>

395

396 Martinez, M. E., Walton, R. D., Bayer, J. D., Haïssaguerre, M., Vigmond, E. J., Hocini, M., & Bernus, O.

397 (2018). Role of the Purkinje-Muscle Junction on the Ventricular Repolarization Heterogeneity in the Healthy and

- 398 Ischemic Ovine Ventricular Myocardium. *Frontiers in Physiology*, 9, 718.
399 <https://doi.org/10.3389/fphys.2018.00718>
400
- 401 Nagy, N., Szél, T., Jost, N., Tóth, A., Gy. Papp, J., & Varró, A. (2015). Novel experimental results in human
402 cardiac electrophysiology: Measurement of the Purkinje fibre action potential from the undiseased human heart.
403 *Canadian Journal of Physiology and Pharmacology*, 93(9), 803–810. <https://doi.org/10.1139/cjpp-2014-0532>
404
- 405 Nakayama, K., Suzuki, Y., & Hashimoto, K. (1968). Sustained atrial fibrillation by acetylcholine infusion into
406 the sinus node artery. *The Tohoku Journal of Experimental Medicine*, 96(4), 333–339.
407 <https://doi.org/10.1620/tjem.96.333>
408
- 409 Navarro-Polanco, R. A., Aréchiga-Figueroa, I. A., Salazar-Fajardo, P. D., Benavides-Haro, D. E., Rodríguez-
410 Elías, J. C., Sachse, F. B., Tristani-Firouzi, M., Sánchez-Chapula, J. A., & Moreno-Galindo, E. G. (2013).
411 Voltage sensitivity of M2 muscarinic receptors underlies the delayed rectifier-like activation of ACh-gated K(+) 
412 current by choline in feline atrial myocytes. *The Journal of Physiology*, 591(17), 4273–4286.
413 <https://doi.org/10.1113/jphysiol.2013.255166>
414
- 415 Nobles, M., Montaigne, D., Sebastian, S., Birnbaumer, L., & Tinker, A. (2018). Differential effects of inhibitory
416 G protein isoforms on G protein-gated inwardly rectifying K⁺ currents in adult murine atria. *American Journal*
417 *of Physiology. Cell Physiology*, 314(5), C616–C626. <https://doi.org/10.1152/ajpcell.00271.2016>
418
- 419 Pappano, A. J., & Carmeliet, E. E. (1979). Epinephrine and the pacemaking mechanism at plateau potentials in
420 sheep cardiac Purkinje fibers. *Pflugers Archiv: European Journal of Physiology*, 382(1), 17–26.
421 <https://doi.org/10.1007/BF00585899>
422
- 423 Recordati, G., Schwartz, P. J., Pagani, M., Malliani, A., & Brown, A. M. (1971). Activation of cardiac vagal
424 receptors during myocardial ischemia. *Experientia*, 27(12), 1423–1424. <https://doi.org/10.1007/BF02154267>
425
- 426 Song, Y., Thedford, S., Lerman, B. B., & Belardinelli, L. (1992). Adenosine-sensitive afterdepolarizations and
427 triggered activity in guinea pig ventricular myocytes. *Circulation Research*, 70(4), 743–753.
428 <https://doi.org/10.1161/01.res.70.4.743>
429

- 430 Terzic, A., Tung, R. T., Inanobe, A., Katada, T., & Kurachi, Y. (1994). G proteins activate ATP-sensitive K⁺
431 channels by antagonizing ATP-dependent gating. *Neuron*, 12(4), 885–893. [https://doi.org/10.1016/0896-](https://doi.org/10.1016/0896-6273(94)90340-9)
432 [6273\(94\)90340-9](https://doi.org/10.1016/0896-6273(94)90340-9)
433
- 434 Trandum-Jensen, J., Wilde, A. A., Vermeulen, J. T., & Janse, M. J. (1991). Morphology of electrophysiologically
435 identified junctions between Purkinje fibers and ventricular muscle in rabbit and pig hearts. *Circulation*
436 *Research*, 69(2), 429–437. <https://doi.org/10.1161/01.res.69.2.429>
437
- 438 Vajda, S., Baczkó, I., & Leprán, I. (2007). Selective cardiac plasma-membrane K(ATP) channel inhibition is
439 defibrillatory and improves survival during acute myocardial ischemia and reperfusion. *European Journal of*
440 *Pharmacology*, 577(1–3), 115–123. <https://doi.org/10.1016/j.ejphar.2007.08.016>
441
- 442 Varró, A., & Baczkó, I. (2010). Possible mechanisms of sudden cardiac death in top athletes: A basic cardiac
443 electrophysiological point of view. *Pflügers Archiv: European Journal of Physiology*, 460(1), 31–40.
444 <https://doi.org/10.1007/s00424-010-0798-0>
445
- 446 Varro, A., Baláti, B., Iost, N., Takács, J., Virág, L., Lathrop, D. A., Csaba, L., Tálosi, L., & Papp, J. G. (2000).
447 The role of the delayed rectifier component I_{Ks} in dog ventricular muscle and Purkinje fibre repolarization. *The*
448 *Journal of Physiology*, 523 Pt 1, 67–81. <https://doi.org/10.1111/j.1469-7793.2000.00067.x>
449
- 450 Weiss, J. N., & Venkatesh, N. (1993). Metabolic regulation of cardiac ATP-sensitive K⁺ channels.
451 *Cardiovascular Drugs and Therapy*, 7 Suppl 3, 499–505. <https://doi.org/10.1007/BF00877614>
452
- 453 Zuanetti, G., De Ferrari, G. M., Priori, S. G., & Schwartz, P. J. (1987). Protective effect of vagal stimulation on
454 reperfusion arrhythmias in cats. *Circulation Research*, 61(3), 429–435. <https://doi.org/10.1161/01.res.61.3.429>

Figure Legends

Figure 1. Representative traces of Purkinje fiber (A, B) and ventricular muscle preparations (C, D); 5 μ M acetylcholine (red dotted lines) alone caused no changes in either preparation type (A, C), while it caused significant prolongation when applied cumulatively after 5 μ M pinacidil (B, D, pinacidil effect represented as blue dashed lines). Bars in panel E represent the values of APD₉₀ in each treatment group, from top to bottom corresponding to the traces A to D. Abbreviations under bars: C, control; P, pinacidil, A, acetylcholine. The pacing cycle length was 500 ms. Values are mean \pm SEM; *,# $p < 0.05$ RM-ANOVA followed by Bonferroni's post-hoc test.

Figure 2. Pinacidil (5 μ M) increased the action potential duration dispersion (indicated by Δ APD₉₀ in percentages, and in ms above the bars) between Purkinje fiber and ventricular muscle preparations, while acetylcholine (5 μ M), when applied after pinacidil, decreased dispersion. The pacing cycle length was 500 ms.

Figure 3. Effect of carbachol on I_{K-ATP} . Ionic currents were measured under a slow voltage ramp protocol (panel A) between -120 mV and 60 mV. The currents were analysed at 0 and 30 mV. Panel B demonstrates original representative current traces (left) and bar graphs (right) where 3 μ M carbachol (dotted line) failed to influence the control current analysed at 0 mV. Inset shows identical current fractions between -3 mV and 45 mV (indicated by dashed rectangle). Current traces in panel C as well as in the inset, illustrate large increase of the membrane current after application of 5 μ M pinacidil (blue dashed line) that was inhibited by the subsequently applied 3 μ M carbachol (red dotted line). In bar graphs (right), asterisk denotes significant change between control (left column) and pinacidil (middle column), while hash tag indicates significant change between pinacidil (middle column) and carbachol (right column).

Figure 4. Representative action potential trace (A) showing that hypoxic conditions caused significant action potential duration abbreviation and decreased mean diastolic potential and amplitude in canine ventricular preparations (blue dashed line), while acetylcholine (5 μ M) caused a significant prolongation in action potential duration (red dotted line). Values of APD₉₀ are represented as bars (B). Abbreviations under bars: C, control; H, hypoxia, A, acetylcholine. The pacing cycle length was 500 ms. Values are mean \pm SEM; *,#p<0.05, RM-ANOVA followed by Bonferroni's post-hoc test.

Figure 5. Representative action potential showing the effect of acetylcholine (5 μ M, red dotted line) on a Purkinje fiber taken from a human donor heart (A). Values of APD₉₀ are represented as bars (B). Abbreviations under bars: C, control; A, acetylcholine. The pacing cycle length was 500 ms. Values are mean \pm SEM.

**Muscarinic agonists inhibit the ATP-dependent potassium current and suppress the
ventricle-Purkinje action potential dispersion**

Tibor Magyar^{a,§}, Tamás Árpádfy-Lovas^{a,§}, Bence Pásztai^a, Noémi Tóth^a, Jozefina Szlovák^a,
Péter Gazdag^a, Zsófia Kohajda^b, András Gyökeres^a, Balázs Györe^d, Zsolt Gurabi^a, Norbert
Jost^{a,b,c}, László Virág^{a,c}, Julius Gy. Papp^{a,b}, Norbert Nagy^{a,b,#}, István Koncz^{a,*,#}

^aDepartment of Pharmacology and Pharmacotherapy, Faculty of Medicine, University of
Szeged, Szeged, Hungary;

^bMTA-SZTE Research Group of Cardiovascular Pharmacology, Hungarian Academy of
Sciences, Szeged, Hungary

^cDepartment of Pharmacology and Pharmacotherapy, Interdisciplinary Excellence Centre,
University of Szeged, Szeged, Hungary

^dFaculty of Dentistry, University of Szeged, Hungary

[§] Shared first authorship

[#] Shared senior authorship

*Author for correspondence at:

István Koncz MD, PhD

Department of Pharmacology & Pharmacotherapy

Faculty of Medicine

University of Szeged

Dóm tér 12,

H-6720 Szeged, Hungary

E-mail: koncz.istvan@med.u-szeged.hu

Abstract

Introduction: Activation of the parasympathetic nervous system has been reported to have an antiarrhythmic role during ischemia-reperfusion injury by decreasing the arrhythmia triggers. Furthermore, it was reported that the parasympathetic neurotransmitter acetylcholine is able to modulate the ATP-dependent K-current (I_{K-ATP}), a crucial current activated during hypoxia. However, the possible significance of this current modulation in the antiarrhythmic mechanism is not fully clarified.

Methods: Action potentials were measured using the conventional microelectrode technique from canine left ventricular papillary muscle and free-running Purkinje fibers, under normal and hypoxic conditions. Ionic currents were measured using the whole-cell configuration of the patch clamp method.

Results: 5 μ M acetylcholine did not influence the action potential duration (APD) either in Purkinje fibers or in papillary muscle preparations. In contrast, it significantly lengthened the APD and suppressed the Purkinje–ventricle APD dispersion when it was administered after 5 μ M pinacidil application. 3 μ M carbachol reduced the pinacidil-activated I_{K-ATP} under voltage-clamp condition. Acetylcholine lengthened the ventricular action potential under simulated ischemia condition.

Conclusion: In this study we found that acetylcholine inhibits the I_{K-ATP} and thus suppresses the ventricle-Purkinje APD dispersion. We conclude that parasympathetic tone may reduce the arrhythmogenic substrate exerting a complex antiarrhythmic mechanism during hypoxic conditions.

Key words: acetylcholine, Purkinje fibers, papillary muscles, hypoxia

Introduction

The parasympathetic nervous system has a crucial role in controlling the actual heart rate and impulse propagation via influencing the sinoatrial and atrioventricular nodes (Higgins et al., 1973). The parasympathetic nerve endings operate by releasing acetylcholine that acts on M_2 -receptors, activating several intracellular signaling routes, and ultimately influencing the cardiac ion channels (Harvey and Belevych, 2003). Even though the parasympathetic nervous system primarily innervates the supraventricular areas of the heart, there are certain important ion channels in the ventricular muscle that are known to be influenced by the release of acetylcholine. It has been previously reported that the inward rectifier potassium current (I_{K1} ; Koumi et al., 1995) and the slow component of the delayed rectifier (I_{Ks} ; Pappano and Carmeliet, 1979) are inhibited, whereas I_{K-ATP} and I_{K-ACh} are activated by acetylcholine via G proteins (Terzic et al, 1994; Ito et al., 1994; Kim et al., 1997).

The importance of these effects of acetylcholine is underpinned by the fact that the activation of I_{K-ATP} channels is well known during hypoxia/ischemia, in which situations the duration of the action potential is shortened (Weiss and Venkatesh, 1993). Furthermore, it was reported that vagal activation is also facilitated under ischemia–reperfusion (Recordati et al., 1971). This vagal activation during hypoxia could be antiarrhythmic, since it was reported that increased parasympathetic tone reduces the catecholaminerg-induced early and delayed afterdepolarizations (arrhythmia triggers) (Song et al., 1992), as well as the incidence of ventricular fibrillation (Zuanetti et al., 1987; Collins and Billman, 1989). However, the underlying mechanism of antiarrhythmic effect of M_2 -receptor activation is not fully clarified. Arrhythmias may develop when an arrhythmogenic substrate (e. g., dispersion of repolarization) and arrhythmia triggers (e.g.: early and delayed afterdepolarizations) simultaneously exist in the heart. The arrhythmogenic substrate could be prominent at Purkinje–ventricle connection because of the relatively weak electrotonic coupling due to low number of gap junctions (Varró and Baczkó, 2010). As a consequence of the different

pharmacological susceptibility of Purkinje fiber and ventricular muscle (Baláti et al, 1998), the activation of I_{K-ATP} may modulate the Purkinje and ventricular action potential duration (APD) to different extents, and the developed APD dispersion may contribute to the onset of arrhythmias.

The objective of this study was the investigation of the possible effect of acetylcholine on the I_{K-ATP} and on the I_{K-ATP} -mediated action potential dispersion under normal and hypoxic conditions.

Methods

Human tissues

Non-diseased human hearts that were unusable for transplantation (based on logistical, not patient-related considerations) were obtained from organ donors. Before cardiac explantation, organ donor patients did not receive medication except dobutamine, furosemide and plasma expanders. The investigations conform to the principles outlined in the *Declaration of Helsinki* of the World Medical Association. All experimental protocols were approved by the Scientific and Research Ethical Committee of the Medical Scientific Board at the Hungarian Ministry of Health (ETT-TUKEB), under ethical approval No 4991-0/2010-1018EKU (339/PI/010). Human cardiac tissue was stored in cardioplegic solution at 4°C for 4–8 hours.

Animals

All experiments using canine cardiac preparations were carried out in compliance with the Guide for the Care and Use of Laboratory Animals (USA NIH publication NO 85-23, revised 1996) and conformed to the Directive 2010/63/EU of the European Parliament. The protocols have been approved by the Ethical Committee for the Protection of Animals in Research of the University of Szeged, Szeged, Hungary (approval number: I-74-24-2017) and by the

Department of Animal Health and Food Control of the Ministry of Agriculture and Rural Development (authority approval number XIII/3331/2017).

Conventional microelectrode technique

Ventricular (papillary or trabecular) muscles were obtained from the right ventricle of canine hearts. Free-running Purkinje fibers were identified as false tendons and isolated from both ventricles of human and canine hearts. Canine hearts were removed through a right lateral thoracotomy from anesthetized (thiopental 30 mg/kg i.v.) mongrel dogs of either sex weighing 10–15 kg. At impalement, Purkinje fibers were observed under a surgical microscope (Zeiss OPMI PRO). The preparations were placed in Locke's solution and allowed to equilibrate for at least 2 hours while superfused (flow rate 4-5 ml/min) also with Locke's solution containing (in mM): NaCl 120, KCl 4, CaCl₂ 2, MgCl₂ 1, NaHCO₃ 22, and glucose 11. The pH of this solution was 7.40 to 7.45 when gassed with 95% O₂ and 5% CO₂ at 37 °C. In the experiments where the effects of tissue hypoxia were examined, we changed the gas mixture to 95% N₂ and 5% CO₂, pH remained at 7.40 to 7.45. All experiments were performed at 37 °C. During the equilibration period, preparations were stimulated at a basic cycle length of 500 ms. Electrical pulses of 0.5–2 ms in duration at twice the diastolic threshold in intensity (S₁) were delivered to the preparations through bipolar platinum electrodes. Transmembrane potentials were recorded using glass capillary microelectrodes filled with 3 M KCl (tip resistance: 5 to 15 MΩ). The microelectrodes were coupled through an Ag-AgCl junction to the input of a high-impedance, capacitance-neutralizing amplifier (Experimetria 2011). Intracellular recordings were displayed on a storage oscilloscope (Hitachi V-555) and led to a computer system (APES) designed for on-line determination of the following parameters: resting membrane potential, action potential amplitude, action potential duration at 10% to 90% repolarization and the maximum rate of rise of the action potential upstroke (V_{max}). Control recordings were obtained after equilibration period. The compounds used in all experiments were purchased from Sigma/Merck.

2.3. Cell isolation

Ventricular myocytes were enzymatically dissociated from the left ventricle of dog hearts. Canine hearts were removed through a right lateral thoracotomy from anesthetized (thiopental 30 mg/kg i.v.) mongrel dogs of either sex weighing 10–15 kg. Cardiac myocytes were isolated from the left ventricle, containing an arterial branch through which the segment was perfused on a Langendorff apparatus with solutions in the following sequence: normal Tyrode's solution (containing in mM: 144 mM NaCl, 0.4 mM NaH₂PO₄, 4 mM KCl, 0.53 mM MgSO₄, 1.8 mM CaCl₂, 5.5 mM Glucose, 5 mM HEPES, pH 7.4 adjusted with NaOH) for 10 min, Ca²⁺-free Tyrode solution for 10 min and Ca²⁺-free Tyrode solution containing collagenase (Worthington type II, 0.66 mg/mL). To the final perfusion solution protease (type XIV, 0.12 mg/mL) was added at the 15 and the 30 minutes for digestion.

2.4. Measurement of ionic currents

One drop of cell suspension was placed in a transparent recording chamber mounted on the stage of an inverted microscope (Olympus IX51, Tokyo, Japan), and individual myocytes were allowed to settle and adhere to the chamber bottom for at least 5–10 min before superfusion was initiated and maintained by gravity. Only rod-shaped cells with clear striations were used. HEPES-buffered Tyrode's solution (composition in mM: NaCl 144, NaH₂PO₄ 0.4, KCl 4.0, CaCl₂ 1.8, MgSO₄ 0.53, glucose 5.5 and HEPES 5.0, at pH of 7.4) was used as the normal superfusate. During the measurement of I_{K-ATP} , 1 μ M nisoldipine was added to the bath solution to block I_{CaL} , I_{Kr} was blocked by 0.1 μ M dofetilide, and I_{Ks} was blocked by 0.5 μ M HMR-1556. Micropipettes were fabricated from borosilicate glass capillaries (Science Products GmbH, Hofheim, Germany), using a P-97 Flaming/Brown micropipette puller (Sutter Co, Novato, CA, USA), and had a resistance of 1.5–2.5 M Ω when filled with pipette solution. The membrane currents were recorded with Axopatch-200B amplifiers (Molecular Devices, Sunnyvale, CA, USA) by applying the whole-cell configuration of the patch-clamp technique. The membrane currents were digitized with 250

kHz analogue to digital converters (Digidata 1440A, Molecular Devices, Sunnyvale, CA, USA) under software control (pClamp 8 and pClamp 10, Molecular Devices, Sunnyvale, CA, USA). The composition of the pipette solution (in mM) was the following: KOH 110, KCl 40, K₂ATP 5, MgCl₂ 5, EGTA 5, HEPES 10 and GTP 0.1 (pH was adjusted to 7.2 by aspartic acid).

2.5 Statistical analysis

Results are expressed as mean ± S.E.M. Normality of distributions was verified using Shapiro-Wilk test, and homogeneity of variances was verified using Bartlett's test in each treatment group. Statistical comparisons were made using analysis of variance (ANOVA) for repeated measurements, followed by Bonferroni's post-hoc test. Differences were considered significant when $p < 0.05$.

Results

1. Acetylcholine lengthened the APD after pinacidil-mediated action potential shortening

Canine Purkinje fibers and ventricular papillary muscles were paced at 500 ms cycle length. In canine Purkinje fibers (PFs; n=15), acetylcholine (5 μM) did not affect the repolarization (233.6±4.7 to 231.7±4.6; Figures 1A and 1E). In contrast, in canine Purkinje fibers (n=8), the I_{K-ATP} activator pinacidil, applied in 5 μM concentration, significantly abbreviated APD₉₀ (207.7±7.0 ms vs 113.1±9.1 ms, $p<0.05$) values. After steady state was reached, acetylcholine was administered. Within 3 minutes, acetylcholine prolonged APD₉₀ to 147.3±7.4 ms, partially reversing the effects of pinacidil (Figures 1B and 1E; $p<0.05$).

Similarly, as observed in Purkinje fibers, 5 μM acetylcholine alone failed to influence the APD of the ventricular muscle (APD₉₀: 172.6±5.7 ms vs 172.8±5.3 ms). Pinacidil (n=5; 5 μM) pretreatment significantly abbreviated the APD₉₀ value (187.9±4.5 ms vs 163.7±6.4 ms, $p<0.05$), similarly to the effects observed in the case of PFs. After a period of

30 minutes, sufficient to reach a steady state, acetylcholine was added to the superfusate. Within 4 minutes, acetylcholine ($5\ \mu\text{M}$) prolonged APD_{90} to $172.1 \pm 7.4\ \text{ms}$ ($p < 0.05$), thus partially reversing the effects of pinacidil (Figures 1D and 1E).

2. *Acetylcholine decreased the calculated APD dispersion between PF and VM*

The changes in the difference between the APD_{90} values of PF and VM can be used to infer the effects of pinacidil and acetylcholine on the dispersion between these cardiac tissue types (Figure 2). The control APD_{90} dispersion (9.5%, 20 ms) was significantly increased upon $5\ \mu\text{M}$ pinacidil application (44.7%, 51 ms). On the other hand, subsequently applied $5\ \mu\text{M}$ acetylcholine markedly decreased the repolarization heterogeneity (16.9%, 28 ms; $p < 0.05$).

3. *Carbachol decreased the pinacidil-induced current activation*

During ionic current measurements, voltage ramps were used from a holding potential of $-90\ \text{mV}$. Membrane potential was hyperpolarized to $-120\ \text{mV}$, and then was slowly (over 36 s) depolarized to $60\ \text{mV}$. Ionic currents were analyzed and compared at 0 and $+30\ \text{mV}$. We found that carbachol did not change the control current when it was applied *without* pinacidil ($0\ \text{mV}$ - control: $0.20 \pm 0.2\ \text{pA/pF}$ vs $3\ \mu\text{M}$ carbachol: $0.32 \pm 0.2\ \text{pA/pF}$, $n=6$ and $+30\ \text{mV}$ - control: $0.55 \pm 0.4\ \text{pA/pF}$ vs $3\ \mu\text{M}$ carbachol: $0.74 \pm 0.3\ \text{pA/pF}$, $n=6$). In contrast, when $5\ \mu\text{M}$ pinacidil was applied first, subsequently employed carbachol significantly reduced the current at both voltages ($0\ \text{mV}$ - control: $0.24 \pm 0.2\ \text{pA/pF} \rightarrow 5\ \mu\text{M}$ pinacidil: $2.03 \pm 0.3\ \text{pA/pF} \rightarrow 3\ \mu\text{M}$ carbachol: $1.51 \pm 0.4\ \text{pA/pF}$, $n=8$, $p < 0.05$. $+30\ \text{mV}$ - control: $0.78 \pm 0.6\ \text{pA/pF} \rightarrow 5\ \mu\text{M}$ pinacidil: $3.17 \pm 0.3\ \text{pA/pF} \rightarrow 3\ \mu\text{M}$ carbachol: $2.26 \pm 0.3\ \text{pA/pF}$, $n=8$, $p < 0.05$).

These measurements were carried out with acetylcholine as well. However, we found carbachol to be more stable during the applied long voltage protocol.

211 *4. Acetylcholine restored the APD after hypoxia-induced action potential shortening*

212 Simulated hypoxia, achieved by gassing the solution with N₂ and CO₂ instead of O₂ and CO₂,
213 resulted in a significant abbreviation of APD₉₀ from 181.4±5.7 ms to 135.0±8.6 ms (p<0.05,
214 Figures 4A and 4B), and a decrease in amplitude (103.7±2.8 mV vs 92±3.5 mV). The
215 maximum rate of depolarization was also decreased (185.8±15.8 V/s vs 156.1±20.6 V/s).
216 When applied during hypoxia, 5 µM acetylcholine caused a significant APD₉₀ prolongation to
217 164.4±4.4 ms, partially reversing the effect of hypoxia on the repolarization. AMP returned to
218 a normal range (102.1±1.6 mV), while V_{max} remained at 156.0±16.1 V/s.

220 *5. Acetylcholine caused a slight abbreviation in human Purkinje fibers*

221 In human PFs (n=2), acetylcholine in 5 µM concentration caused a slight abbreviation of
222 APD₉₀ from 269.0±28.4 to 251.6±42.85 ms and APD₅₀ from 184.4±20.0 ms to
223 173.3±27.1 ms without affecting other characteristics of the action potential (Figure 5).

225 **Discussion**

226 In this study we investigated the electrophysiological effects of muscarinic agonists on the
227 I_{K-ATP} current. We found that (i) under normal conditions acetylcholine did not influence the
228 action potential duration. (ii) In contrast, when I_{K-ATP} was pharmacologically activated by
229 pinacidil, subsequently applied acetylcholine lengthened the action potential duration as well
230 as (iii) reduced the pinacidil-induced ventricle-Purkinje APD dispersion. (iv) In line with this,
231 carbachol inhibited the I_{K-ATP} that was previously activated by pinacidil. (v) Acetylcholine
232 increased the APD after hypoxia-induced action potential shortening.

234 *Acetylcholine inhibits the I_{K-ATP} in canine ventricular myocytes*

235 It is well known that acetylcholine shortens the atrial APD and has been implicated in atrial
236 fibrillation (Nakayama et al, 1968). Acetylcholine directly affects the GIRK1/4 or
237 Kir3.1/Kir3.4 channels (Nobles et al, 2018; Corey and Clapham, 1998), encoded by *KCNJ3*

and *KCNJ4* genes (Kurachi, 1995). These channels are largely expressed in atrial, SA and AV nodal cells (Galindo et al, 2016; Navarro-Polanco et al, 2013). At the same time, previous studies (Terzic et al, 1994; Ito et al., 1994) claimed that acetylcholine activates the I_{K-ATP} channels, even though the physiological consequences of this effect on the action potential were not clarified.

The I_{K-ATP} ATP-sensitive potassium channels comprise hetero-octamers consisting of four inward rectifying potassium channel pore-forming subunits (Kir6.1 or Kir6.2, encoded by *KCNJ8* and *KCNJ11* genes, respectively) and four ATP-binding cassette protein sulphonylurea receptors (SUR1 or SUR2, encoded by *ABCC8* and *ABCC9* genes, respectively; Inagaki et al, 1995). An important feature of the I_{K-ATP} is its closed state under physiological intracellular ATP levels (i. e., under normoxia) and its activation by metabolic stress, when the ratio of ATP/ADP is decreased, e. g., during myocardial ischemia (Deutsch et al., 1991).

Activation of the sarcolemmal I_{K-ATP} during myocardial ischemia shortens the action potential of various cardiac tissues to different extents, thus it may promote APD dispersion and re-entry type arrhythmias (Janse and Wit, 1989). Accordingly, several investigations found I_{K-ATP} activation to be pro-arrhythmic (Chi et al., 1990), suggesting that sarcolemmal I_{K-ATP} inhibition may prevent arrhythmias induced by myocardial ischemia and ischemia/reperfusion (Billman et al, 1998; Englert et al, 2003; Vajda et al, 2007).

In our experiments under normal conditions, we found no effect of carbachol on the membrane current (Figure 3) and, similarly, acetylcholine failed to influence the ventricular and Purkinje APDs (Figures 1A and 1C). The observed discrepancy between our and previous results, where an activation of I_{K-ATP} was described upon acetylcholine administration (Terzic

et al, 1994; Ito et al, 1994; Kim et al., 1997), could be the consequence of the species difference and the distinct experimental conditions.

In contrast, an important, and, to the best of our knowledge, previously not published result of our study is that carbachol is able to suppress the pinacidil-activated I_{K-ATP} . As a consequence, in parallel tissue action potential experiments, acetylcholine lengthened the APD as long as it was previously shortened by the application of I_{K-ATP} -activator pinacidil. Since I_{K-ATP} activation could be arrhythmogenic (Chi et al., 1990) by causing an increase in the APD dispersion, this effect of acetylcholine raises the possibility of a novel antiarrhythmic mechanism of the previously described antiarrhythmic effect of parasympathetic activation during hypoxia (Song et al., 1992; Zuanetti et al., 1987; Collins and Billman, 1989).

Our experiments conducted under hypoxic conditions provided similar results (i. e., acetylcholine lengthened the hypoxia-induced shortened ventricular action potential; Figure 4). Even though tissue hypoxia is a complex phenomenon (Carmeliet, 1999), during which several factors change simultaneously (e. g., Ca^{2+}_i , Na^+_i , pH, conductance of gap junctions, membrane potential etc.), it is feasible that I_{K-ATP} activation, as a response to ATP depletion, is an important factor in the observed action potential shortening. Since acetylcholine lengthened the action potential under hypoxic conditions, we suggest I_{K-ATP} inhibition as a possible underlying mechanism.

Acetylcholine decreased the pinacidil-induced ventricle–Purkinje APD dispersion

Free-running Purkinje fibers connect to the ventricular muscle on a small surface area, providing a relatively large-resistance coupling (Tranum-Jensen et al., 1991), and a large sink for current flow that favors conduction blocks more than other parts of the healthy myocardium. Also, due to the weaker electrotonic coupling, the dispersion of repolarization here can be greater than in other areas (Martinez et al., 2018), causing the Purkinje–ventricle

APD ratio to have critical importance in arrhythmia generation. In our experiments, we found significantly greater shortening in Purkinje fibers caused by pinacidil that could be the consequence of the generally weaker repolarization reserve that makes the Purkinje action potential to be more susceptible to any pharmacological interventions (Varró et al, 2000; Baláti et al, 1998). Similarly, acetylcholine exerted larger lengthening in the Purkinje fiber probably by the same reason that ultimately led to reduced ventricle–Purkinje APD dispersion. The reduction of the ventricle–Purkinje fiber APD dispersion could suppress the arrhythmogenic substrate providing a narrower vulnerable period for a critically timed extrasystole to trigger a life-threatening arrhythmia under hypoxic conditions.

Proposed mechanism

Since inhibition of the I_{K-ATP} channels is possible by blocking various PKA-mediated pathways (Tinker et al, 2018.), we suggest that the decrease of cAMP levels caused by the activation of cardiac muscarinic receptors using acetylcholine/carbachol was the factor that decreased the density of the I_{K-ATP} current in patch clamp measurements, leading to the subsequent prolongation observed in action potential durations.

Conclusions

We found that muscarinic agonists inhibit the I_{K-ATP} . Therefore, during I_{K-ATP} -mediated action potential shortening, acetylcholine causes asymmetrical action potential lengthening between ventricular muscle and Purkinje fiber that leads to reduced APD dispersion.

These results suggest that the parasympathetic tone beyond suppressing the catecholaminerg-induced arrhythmogenic triggers (Song et al., 1992) may be also able to reduce the arrhythmogenic substrate under hypoxic conditions.

Study Limitations

(i) In our experiments, the ventricular and Purkinje fiber action potentials were measured from electrically uncoupled tissue samples.

(ii) The presented effects were attributed to the M2 muscarinic receptor; nevertheless, the exact level of contribution of other receptor subtypes was not addressed. To achieve this, further studies are needed, utilizing specific agonist and antagonist drugs.

Acknowledgments

We are grateful to Dr. Károly Acsai for his valuable contribution in performing statistical comparisons. This work was supported by grants from the National Research, Development and Innovation Office – NKFIH PD-116011 (for IK), FK-129117 (for NN) and the ÚNKP-18-4, 19-4 and ÚNKP-20-5-SZTE-165 New National Excellence Program of the Ministry for Innovation and Technology (for IK and NN), the János Bolyai Research Scholarship of the Hungarian Academy of Sciences (for NN) and EFOP-3.6.2-16-2017-00006 (LIVE LONGER) and EFOP 3.6.3-VEKOP-16-2017-00009 and Ministry of Human Capacities, Hungary grant 20391-3/2018/FEKUSTRAT, and the University of Szeged.

References

- Baláti, B., Varró, A., & Papp, J. G. (1998). Comparison of the cellular electrophysiological characteristics of canine left ventricular epicardium, M cells, endocardium and Purkinje fibers. *Acta Physiologica Scandinavica*, 164(2), 181–190. <https://doi.org/10.1046/j.1365-201X.1998.00416.x>
- Billman, G. E., Englert, H. C., & Schölkens, B. A. (1998). HMR 1883, a novel cardioselective inhibitor of the ATP-sensitive potassium channel. Part II: Effects on susceptibility to ventricular fibrillation induced by myocardial ischemia in conscious dogs. *The Journal of Pharmacology and Experimental Therapeutics*, 286(3), 1465–1473.
- Carmeliet, E. (1999). Cardiac ionic currents and acute ischemia: From channels to arrhythmias. *Physiological Reviews*, 79(3), 917–1017. <https://doi.org/10.1152/physrev.1999.79.3.917>
- Chi, L., Uprichard, A. C., & Lucchesi, B. R. (1990). Profibrillatory actions of pinacidil in a conscious canine model of sudden coronary death. *Journal of Cardiovascular Pharmacology*, 15(3), 452–464. <https://doi.org/10.1097/00005344-199003000-00016>
- Collins, M. N., & Billman, G. E. (1989). Autonomic response to coronary occlusion in animals susceptible to ventricular fibrillation. *The American Journal of Physiology*, 257(6 Pt 2), H1886–1894. <https://doi.org/10.1152/ajpheart.1989.257.6.H1886>
- Corey, S., & Clapham, D. E. (1998). Identification of native atrial G-protein-regulated inwardly rectifying K⁺ (GIRK4) channel homomultimers. *The Journal of Biological Chemistry*, 273(42), 27499–27504. <https://doi.org/10.1074/jbc.273.42.27499>
- Deutsch, N., Klitzner, T. S., Lamp, S. T., & Weiss, J. N. (1991). Activation of cardiac ATP-sensitive K⁺ current during hypoxia: Correlation with tissue ATP levels. *The American Journal of Physiology*, 261(3 Pt 2), H671–676. <https://doi.org/10.1152/ajpheart.1991.261.3.H671>
- Englert, H. C., Heitsch, H., Gerlach, U., & Knieps, S. (2003). Blockers of the ATP-sensitive potassium channel SUR2A/Kir6.2: A new approach to prevent sudden cardiac death. *Current Medicinal Chemistry. Cardiovascular and Hematological Agents*, 1(3), 253–271. <https://doi.org/10.2174/1568016033477423>

366

367 Harvey, R. D., & Belevych, A. E. (2003). Muscarinic regulation of cardiac ion channels. *British Journal of*
368 *Pharmacology*, 139(6), 1074–1084. <https://doi.org/10.1038/sj.bjp.0705338>

369

370 Higgins, C. B., Vatner, S. F., & Braunwald, E. (1973). Parasympathetic control of the heart. *Pharmacological*
371 *Reviews*, 25(1), 119–155.

372

373 Inagaki, N., Gono, T., Clement, J. P., Namba, N., Inazawa, J., Gonzalez, G., Aguilar-Bryan, L., Seino, S., &
374 Bryan, J. (1995). Reconstitution of IKATP: An inward rectifier subunit plus the sulfonylurea receptor. *Science*
375 *(New York, N.Y.)*, 270(5239), 1166–1170. <https://doi.org/10.1126/science.270.5239.1166>

376

377 Ito, H., Vereecke, J., & Carmeliet, E. (1994). Mode of regulation by G protein of the ATP-sensitive K⁺ channel
378 in guinea-pig ventricular cell membrane. *The Journal of Physiology*, 478 (Pt 1), 101–107.

379 <https://doi.org/10.1113/jphysiol.1994.sp020233>

380

381 Janse, M. J., & Wit, A. L. (1989). Electrophysiological mechanisms of ventricular arrhythmias resulting from
382 myocardial ischemia and infarction. *Physiological Reviews*, 69(4), 1049–1169.

383 <https://doi.org/10.1152/physrev.1989.69.4.1049>

384

385 Kim, D., Watson, M., & Indyk, V. (1997). ATP-dependent regulation of a G protein-coupled K⁺ channel
386 (GIRK1/GIRK4) expressed in oocytes. *The American Journal of Physiology*, 272(1 Pt 2), H195–206.

387 <https://doi.org/10.1152/ajpheart.1997.272.1.H195>

388

389 Koumi, S., Wasserstrom, J. A., & Ten Eick, R. E. (1995). Beta-adrenergic and cholinergic modulation of the
390 inwardly rectifying K⁺ current in guinea-pig ventricular myocytes. *The Journal of Physiology*, 486 (Pt 3), 647–

391 659. <https://doi.org/10.1113/jphysiol.1995.sp020841>

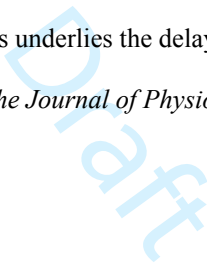
392

393 Kurachi, Y. (1995). G protein regulation of cardiac muscarinic potassium channel. *The American Journal of*
394 *Physiology*, 269(4 Pt 1), C821–830. <https://doi.org/10.1152/ajpcell.1995.269.4.C821>

395

396 Martinez, M. E., Walton, R. D., Bayer, J. D., Haïssaguerre, M., Vigmond, E. J., Hocini, M., & Bernus, O.

397 (2018). Role of the Purkinje-Muscle Junction on the Ventricular Repolarization Heterogeneity in the Healthy and

- 398 Ischemic Ovine Ventricular Myocardium. *Frontiers in Physiology*, 9, 718.
399 <https://doi.org/10.3389/fphys.2018.00718>
400
- 401 Nagy, N., Szél, T., Jost, N., Tóth, A., Gy. Papp, J., & Varró, A. (2015). Novel experimental results in human
402 cardiac electrophysiology: Measurement of the Purkinje fibre action potential from the undiseased human heart.
403 *Canadian Journal of Physiology and Pharmacology*, 93(9), 803–810. <https://doi.org/10.1139/cjpp-2014-0532>
404
- 405 Nakayama, K., Suzuki, Y., & Hashimoto, K. (1968). Sustained atrial fibrillation by acetylcholine infusion into
406 the sinus node artery. *The Tohoku Journal of Experimental Medicine*, 96(4), 333–339.
407 <https://doi.org/10.1620/tjem.96.333>
408
- 409 Navarro-Polanco, R. A., Aréchiga-Figueroa, I. A., Salazar-Fajardo, P. D., Benavides-Haro, D. E., Rodríguez-
410 Elías, J. C., Sachse, F. B., Tristani-Firouzi, M., Sánchez-Chapula, J. A., & Moreno-Galindo, E. G. (2013).
411 Voltage sensitivity of M2 muscarinic receptors underlies the delayed rectifier-like activation of ACh-gated K(+) 
412 current by choline in feline atrial myocytes. *The Journal of Physiology*, 591(17), 4273–4286.
413 <https://doi.org/10.1113/jphysiol.2013.255166>
414
- 415 Nobles, M., Montaigne, D., Sebastian, S., Birnbaumer, L., & Tinker, A. (2018). Differential effects of inhibitory
416 G protein isoforms on G protein-gated inwardly rectifying K⁺ currents in adult murine atria. *American Journal*
417 *of Physiology. Cell Physiology*, 314(5), C616–C626. <https://doi.org/10.1152/ajpcell.00271.2016>
418
- 419 Pappano, A. J., & Carmeliet, E. E. (1979). Epinephrine and the pacemaking mechanism at plateau potentials in
420 sheep cardiac Purkinje fibers. *Pflugers Archiv: European Journal of Physiology*, 382(1), 17–26.
421 <https://doi.org/10.1007/BF00585899>
422
- 423 Recordati, G., Schwartz, P. J., Pagani, M., Malliani, A., & Brown, A. M. (1971). Activation of cardiac vagal
424 receptors during myocardial ischemia. *Experientia*, 27(12), 1423–1424. <https://doi.org/10.1007/BF02154267>
425
- 426 Song, Y., Thedford, S., Lerman, B. B., & Belardinelli, L. (1992). Adenosine-sensitive afterdepolarizations and
427 triggered activity in guinea pig ventricular myocytes. *Circulation Research*, 70(4), 743–753.
428 <https://doi.org/10.1161/01.res.70.4.743>
429

- 430 Terzic, A., Tung, R. T., Inanobe, A., Katada, T., & Kurachi, Y. (1994). G proteins activate ATP-sensitive K⁺
431 channels by antagonizing ATP-dependent gating. *Neuron*, 12(4), 885–893. [https://doi.org/10.1016/0896-](https://doi.org/10.1016/0896-6273(94)90340-9)
432 [6273\(94\)90340-9](https://doi.org/10.1016/0896-6273(94)90340-9)
433
- 434 Trandum-Jensen, J., Wilde, A. A., Vermeulen, J. T., & Janse, M. J. (1991). Morphology of electrophysiologically
435 identified junctions between Purkinje fibers and ventricular muscle in rabbit and pig hearts. *Circulation*
436 *Research*, 69(2), 429–437. <https://doi.org/10.1161/01.res.69.2.429>
437
- 438 Vajda, S., Baczkó, I., & Leprán, I. (2007). Selective cardiac plasma-membrane K(ATP) channel inhibition is
439 defibrillatory and improves survival during acute myocardial ischemia and reperfusion. *European Journal of*
440 *Pharmacology*, 577(1–3), 115–123. <https://doi.org/10.1016/j.ejphar.2007.08.016>
441
- 442 Varró, A., & Baczkó, I. (2010). Possible mechanisms of sudden cardiac death in top athletes: A basic cardiac
443 electrophysiological point of view. *Pflügers Archiv: European Journal of Physiology*, 460(1), 31–40.
444 <https://doi.org/10.1007/s00424-010-0798-0>
445
- 446 Varro, A., Baláti, B., Iost, N., Takács, J., Virág, L., Lathrop, D. A., Csaba, L., Tálosi, L., & Papp, J. G. (2000).
447 The role of the delayed rectifier component I_{Ks} in dog ventricular muscle and Purkinje fibre repolarization. *The*
448 *Journal of Physiology*, 523 Pt 1, 67–81. <https://doi.org/10.1111/j.1469-7793.2000.00067.x>
449
- 450 Weiss, J. N., & Venkatesh, N. (1993). Metabolic regulation of cardiac ATP-sensitive K⁺ channels.
451 *Cardiovascular Drugs and Therapy*, 7 Suppl 3, 499–505. <https://doi.org/10.1007/BF00877614>
452
- 453 Zuanetti, G., De Ferrari, G. M., Priori, S. G., & Schwartz, P. J. (1987). Protective effect of vagal stimulation on
454 reperfusion arrhythmias in cats. *Circulation Research*, 61(3), 429–435. <https://doi.org/10.1161/01.res.61.3.429>

Figure Legends

Figure 1. Representative traces of Purkinje fiber (A, B) and ventricular muscle preparations (C, D); 5 μ M acetylcholine (red dotted lines) alone caused no changes in either preparation type (A, C), while it caused significant prolongation when applied cumulatively after 5 μ M pinacidil (B, D, pinacidil effect represented as blue dashed lines). Bars in panel E represent the values of APD₉₀ in each treatment group, from top to bottom corresponding to the traces A to D. Abbreviations under bars: C, control; P, pinacidil, A, acetylcholine. The pacing cycle length was 500 ms. Values are mean \pm SEM; *,# $p < 0.05$ RM-ANOVA followed by Bonferroni's post-hoc test.

Figure 2. Pinacidil (5 μ M) increased the action potential duration dispersion (indicated by Δ APD₉₀ in percentages, and in ms above the bars) between Purkinje fiber and ventricular muscle preparations, while acetylcholine (5 μ M), when applied after pinacidil, decreased dispersion. The pacing cycle length was 500 ms.

Figure 3. Effect of carbachol on I_{K-ATP} . Ionic currents were measured under a slow voltage ramp protocol (panel A) between -120 mV and 60 mV. The currents were analysed at 0 and 30 mV. Panel B demonstrates original representative current traces (left) and bar graphs (right) where 3 μ M carbachol (dotted line) failed to influence the control current analysed at 0 mV. Inset shows identical current fractions between -3 mV and 45 mV (indicated by dashed rectangle). Current traces in panel C as well as in the inset, illustrate large increase of the membrane current after application of 5 μ M pinacidil (blue dashed line) that was inhibited by the subsequently applied 3 μ M carbachol (red dotted line). In bar graphs (right), asterisk denotes significant change between control (left column) and pinacidil (middle column), while hash tag indicates significant change between pinacidil (middle column) and carbachol (right column).

Figure 4. Representative action potential trace (A) showing that hypoxic conditions caused significant action potential duration abbreviation and decreased mean diastolic potential and amplitude in canine ventricular preparations (blue dashed line), while acetylcholine (5 μ M) caused a significant prolongation in action potential duration (red dotted line). Values of APD₉₀ are represented as bars (B). Abbreviations under bars: C, control; H, hypoxia, A, acetylcholine. The pacing cycle length was 500 ms. Values are mean \pm SEM; *,#p<0.05, RM-ANOVA followed by Bonferroni's post-hoc test.

Figure 5. Representative action potential showing the effect of acetylcholine (5 μ M, red dotted line) on a Purkinje fiber taken from a human donor heart (A). Values of APD₉₀ are represented as bars (B). Abbreviations under bars: C, control; A, acetylcholine. The pacing cycle length was 500 ms. Values are mean \pm SEM.

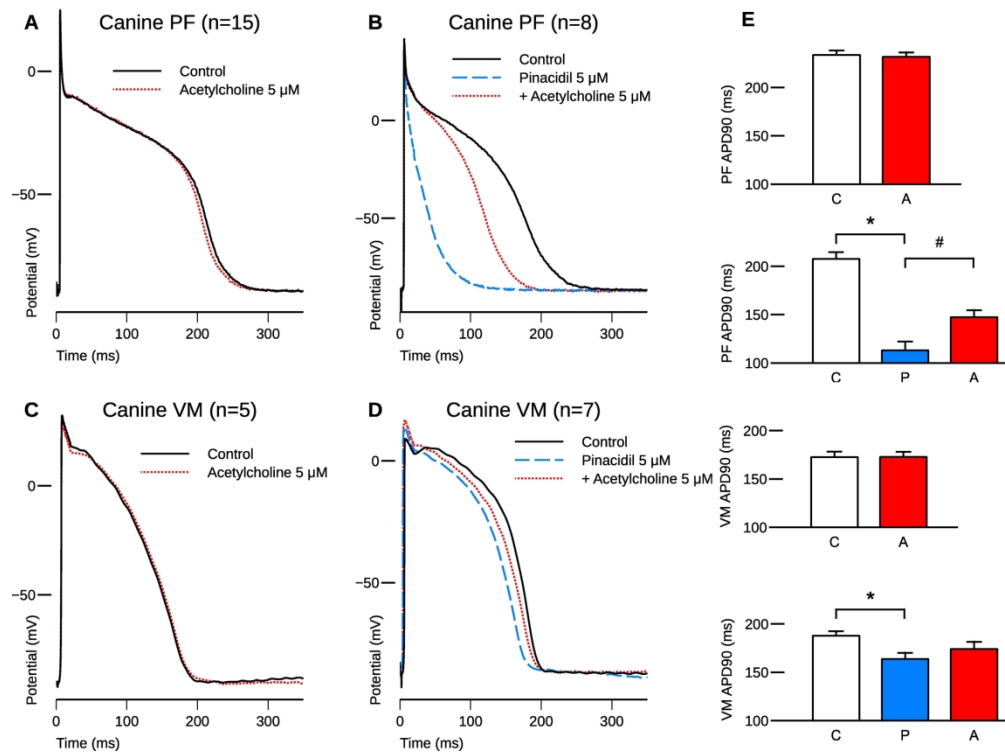


Figure 1. Representative traces of Purkinje fiber (A, B) and ventricular muscle preparations (C, D); 5 μ M acetylcholine (red dotted lines) alone caused no changes in either preparation type (A, C), while it caused significant prolongation when applied cumulatively after 5 μ M pinacidil (B, D, pinacidil effect represented as blue dashed lines). Bars in panel E represent the values of APD90 in each treatment group, from top to bottom corresponding to the traces A to D. Abbreviations under bars: C, control; P, pinacidil, A, acetylcholine. The pacing cycle length was 500 ms. Values are mean \pm SEM; *, # $p < 0.05$ RM-ANOVA followed by Bonferroni's post-hoc test.

207x155mm (300 x 300 DPI)

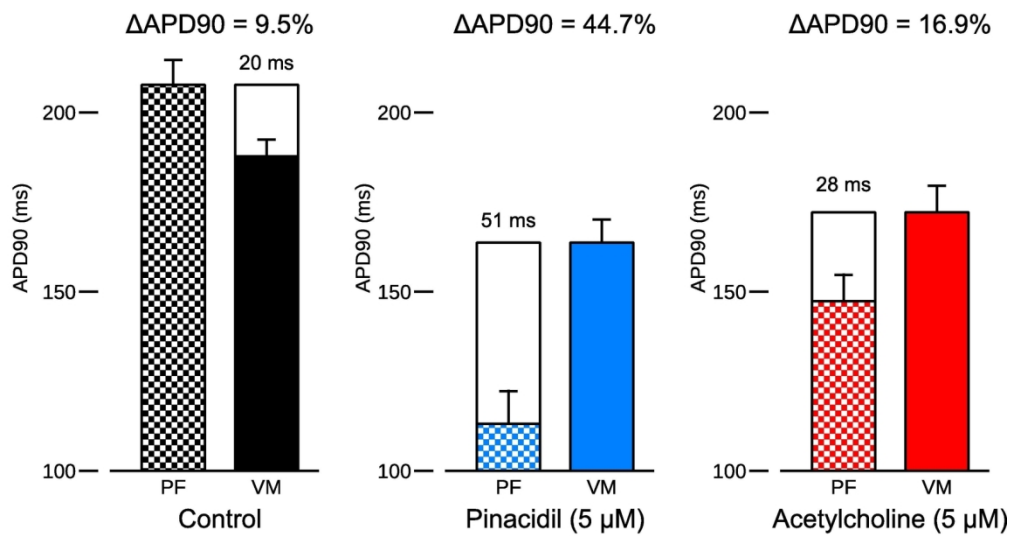


Figure 2. Pinacidil (5 μ M) increased the action potential duration dispersion (indicated by Δ APD90 in percentages, and in ms above the bars) between Purkinje fiber and ventricular muscle preparations, while acetylcholine (5 μ M), when applied after pinacidil, decreased dispersion. The pacing cycle length was 500 ms.

146x79mm (300 x 300 DPI)

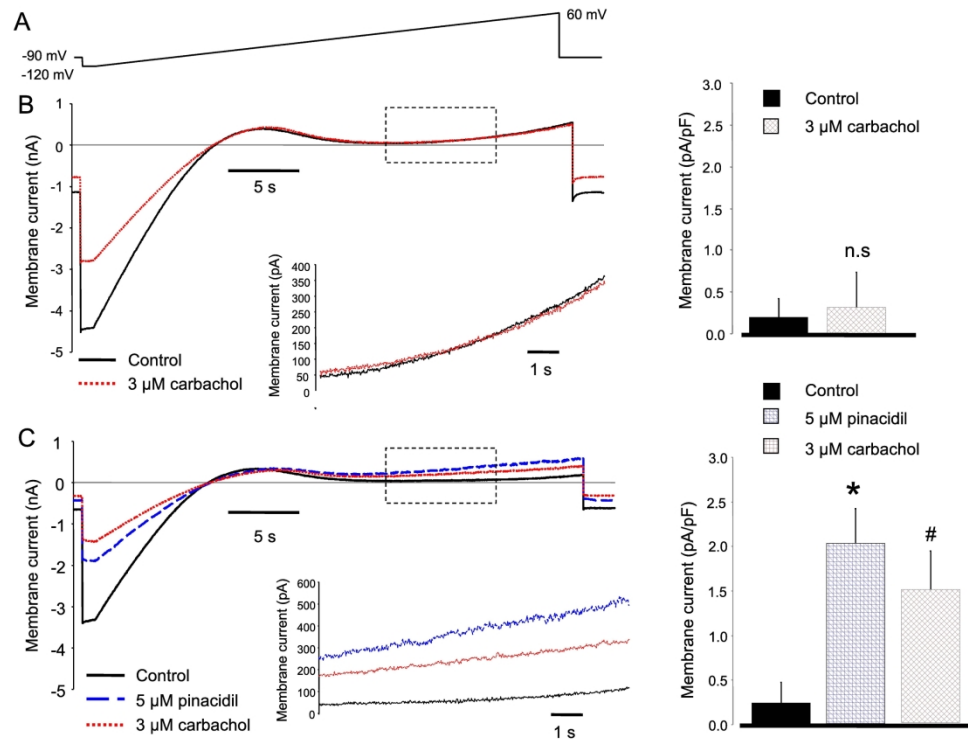


Figure 3. Effect of carbachol on IK-ATP. Ionic currents were measured under a slow voltage ramp protocol (panel A) between -120 mV and 60 mV. The currents were analysed at 0 and 30 mV. Panel B demonstrates original representative current traces (left) and bar graphs (right) where 3 μM carbachol (dotted line) failed to influence the control current analysed at 0 mV. Inset shows identical current fractions between -3 mV and 45 mV (indicated by dashed rectangle). Current traces in panel C as well as in the inset, illustrate large increase of the membrane current after application of 5 μM pinacidil (blue dashed line) that was inhibited by the subsequently applied 3 μM carbachol (red dotted line). In bar graphs (right), asterisk denotes significant change between control (left column) and pinacidil (middle column), while hash tag indicates significant change between pinacidil (middle column) and carbachol (right column).

254x190mm (300 x 300 DPI)

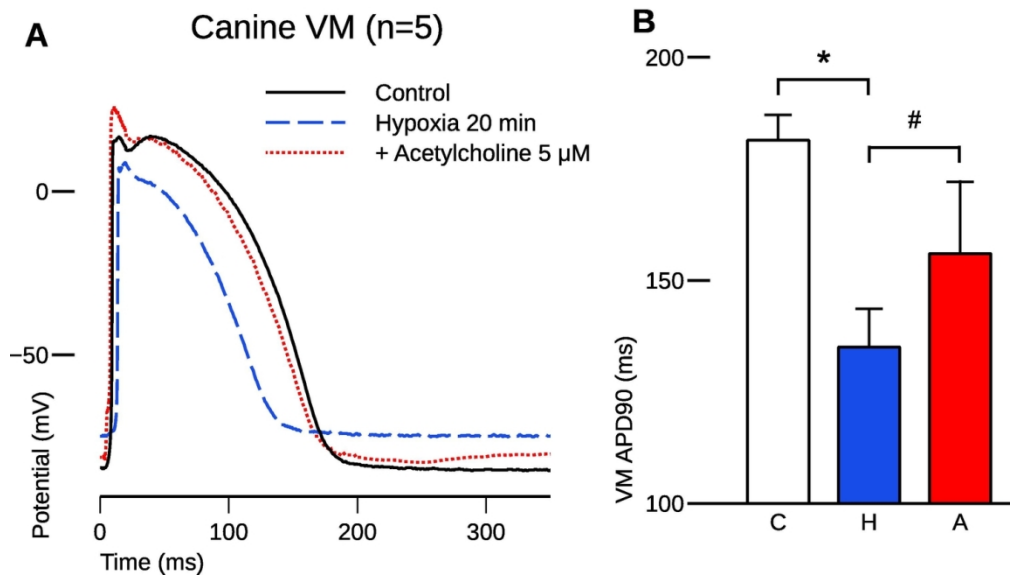


Figure 4. Representative action potential trace (A) showing that hypoxic conditions caused significant action potential duration abbreviation and decreased mean diastolic potential and amplitude in canine ventricular preparations (blue dashed line), while acetylcholine (5 μ M) caused a significant prolongation in action potential duration (red dotted line). Values of APD90 are represented as bars (B). Abbreviations under bars: C, control; H, hypoxia, A, acetylcholine. The pacing cycle length was 500 ms. Values are mean \pm SEM; *,#p<0.05, RM-ANOVA followed by Bonferroni's post-hoc test.

126x74mm (300 x 300 DPI)

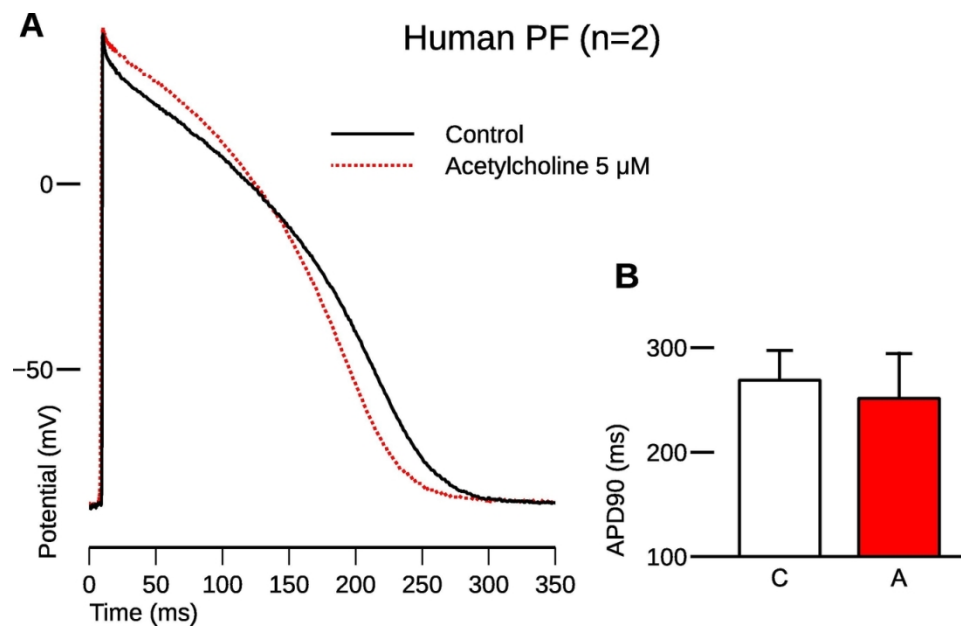


Figure 5. Representative action potential showing the effect of acetylcholine (5 μ M, red dotted line) on a Purkinje fiber taken from a human donor heart (A). Values of APD90 are represented as bars (B). Abbreviations under bars: C, control; A, acetylcholine. The pacing cycle length was 500 ms. Values are mean \pm SEM.

121x74mm (300 x 300 DPI)

1
2
3
4
5
6
7
8
9
10
11

Appendix

Draft

Introduction

Acetylcholine has been previously shown to augment J-point elevation and to induce phase-2 reentry, thus precipitating polymorphic ventricular tachycardia in preparations pretreated with agents designed to pharmacologically mimic the genetic defects previously shown to be associated with the early repolarization syndrome (ERS). Previously, Haïssaguerre et al. (2008) have described that extrasystolic activity arising from the Purkinje network is able to precipitate ventricular tachyarrhythmias in the setting of ERS. We examined Purkinje fibers under conditions pharmacologically mimicking the ion channel changes caused by the genetic defects previously reported to be associated with ERS, including gain of function in I_{K-ATP} (*KCNJ8* and *ABCC9*) or I_{to} (*SCN1Bb* and *KCND3*) (Hu et al., 2014b; Barajas-Martínez et al., 2014; Haïssaguerre et al., 2009) or loss of function in I_{Ca} (*CACNA1C*, *CACNB2* and *CACNA2D1*) (Burashnikov et al., 2010; Napolitano and Antzelevitch, 2011) or I_{Na} (*SCN5A* and *SCN10A*) (Watanabe et al., 2011; Hu et al., 2014a), and applied an antiarrhythmic drug successfully used to treat ventricular tachyarrhythmias in ERS: cilostazol (Iguchi et al., 2013; Shinohara et al., 2014;).

Methods

Conventional microelectrode technique

All experiments were performed on canine Purkinje fibers using the conventional microelectrode technique. The preparations were placed in Locke's solution and allowed to equilibrate for at least 2 hours while superfused (flow rate 4-5 ml/min) also with Locke's solution containing (in mM): NaCl 120, KCl 4, CaCl₂ 2, MgCl₂ 1, NaHCO₃ 22, and glucose 11. The pH of this solution was 7.40 to 7.45 when gassed with 95% O₂ and 5% CO₂ at 37 °C. All experiments were performed at 37 °C. Electrical pulses of 0.5–2 ms in duration at twice the diastolic threshold in intensity (S1) were delivered to the preparations through bipolar platinum electrodes at a basic cycle length of 500 ms. Transmembrane potentials were recorded using glass capillary microelectrodes filled with 3 M KCl (tip resistance: 5 to 15 MΩ). The microelectrodes were coupled through an Ag-AgCl junction to the input of a

37 high-impedance, capacitance-neutralizing amplifier (Experimetria 2011). Intracellular recordings were
38 displayed on a storage oscilloscope (Hitachi V-555) and led to a computer system.

39

40 *Pharmacological models*

41 Our pharmacological models of the early repolarization syndrome in Purkinje fibers were based on
42 previous experiments (Koncz et al., 2014; Gurabi et al., 2014). We pharmacologically mimicked the
43 ion channel changes caused by the genetic defects associated with ERS: pinacidil (5 μ M; I_{K-ATP} gain of
44 function), NS5806 (7 μ M; I_{to} gain of function), nisoldipine (1 μ M; I_{Ca} loss of function), mexiletine
45 (20 μ M; I_{Na} loss of function). The more efficacious enantiomer of mexiletine, R-mexiletine was used
46 (Gurabi et al., 2017); the concentration corresponds to a peak therapeutic plasma concentration (Varró
47 and Lathrop, 1990). The application of each compound was followed by an equilibration period,
48 enabling the tissue to reach steady-state, then the next compound was administered in a cumulative
49 manner. Acetylcholine (5 μ M) was used to simulate increased parasympathetic tone. Cilostazol
50 (10 μ M) was applied after acetylcholine.

51

52 **Results**

53 *Model 1: Pinacidil + acetylcholine + cilostazol (n=6)*

54 The effects of pinacidil and acetylcholine were described in the main article. Cilostazol caused a
55 notable plateau elevation without changing repolarization (Figure A1-A).

56

57 *Model 2: NS5806 + pinacidil + acetylcholine + cilostazol (n=5)*

58 Cilostazol significantly increased action potential duration (APD) when applied after NS5806, pinacidil
59 and acetylcholine (Figure A1-B).

60

61

62 *Model 3: Mexiletine + NS5806 + cilostazol (n=4)*

63 After inhibition of I_{Na} by mexiletine, followed by the activation I_{to} by NS5806 and the administration of
64 acetylcholine, cilostazol caused a slight prolongation of the APD (Figure A1-C).

65

66 *Model 4: Nisoldipine + NS5806 + acetylcholine + cilostazol (n=4)*

67 Cilostazol was also applied after nisoldipine, NS5806 and acetylcholine, causing a slight plateau
68 elevation and slight APD prolongation (Figure A1-D).

69

70 **Conclusion**

71 Since most conventional antiarrhythmic drugs, including beta-blockers, verapamil, lidocaine or
72 amiodarone, are not capable of suppressing tachyarrhythmic episodes in the early repolarization
73 syndrome, cilostazol should remain a prominent candidate in clinical trials related to early
74 repolarization. Formerly, we found I_{to} blocking ability of cilostazol (Patocskai et al., 2016) next to its
75 ability to augment I_{Ca} (Matsui et al., 1999). The above detailed normalization of the repolarization
76 defect might carry a possible therapeutic value of cilostazol in early repolarization (ER), when the
77 origin of arrhythmic activity is localized to the Purkinje system.

78 **References**

- 79 Barajas-Martínez, H., Hu, D., Ferrer, T., Onetti, C. G., Wu, Y., Burashnikov, E., Boyle, M., Surman, T., Urrutia, J.,
80 Veltmann, C., Schimpf, R., Borggrefe, M., Wolpert, C., Ibrahim, B. B., Sánchez-Chapula, J. A., Winters, S., Haïssaguerre,
81 M., & Antzelevitch, C. (2012). Molecular genetic and functional association of Brugada and early repolarization syndromes
82 with S422L missense mutation in KCNJ8. *Heart Rhythm*, 9(4), 548–555. <https://doi.org/10.1016/j.hrthm.2011.10.035>
83
- 84 Burashnikov, E., Pfeiffer, R., Barajas-Martinez, H., Delpón, E., Hu, D., Desai, M., Borggrefe, M., Haïssaguerre, M., Kanter,
85 R., Pollevick, G. D., Guerchicoff, A., Laiño, R., Marieb, M., Nademanee, K., Nam, G.-B., Robles, R., Schimpf, R.,
86 Stapleton, D. D., Viskin, S., ... Antzelevitch, C. (2010). Mutations in the cardiac L-type calcium channel associated with
87 inherited J-wave syndromes and sudden cardiac death. *Heart Rhythm*, 7(12), 1872–1882.
88 <https://doi.org/10.1016/j.hrthm.2010.08.026>
89
- 90 Gurabi, Z., Patocskaï, B., Györe, B., Virág, L., Mátyus, P., Papp, J. G., Varró, A., & Koncz, I. (2017). Different
91 electrophysiological effects of the levo- and dextro-rotatory isomers of mexiletine in isolated rabbit cardiac muscle.
92 *Canadian Journal of Physiology and Pharmacology*, 95(7), 830–836. <https://doi.org/10.1139/cjpp-2016-0599>
93
- 94 Haïssaguerre, M., Chatel, S., Sacher, F., Weerasooriya, R., Probst, V., Loussouarn, G., Horlitz, M., Liersch, R., Schulze-
95 Bahr, E., Wilde, A., Käb, S., Koster, J., Rudy, Y., Le Marec, H., & Schott, J. J. (2009). Ventricular fibrillation with
96 prominent early repolarization associated with a rare variant of KCNJ8/KATP channel. *Journal of Cardiovascular*
97 *Electrophysiology*, 20(1), 93–98. <https://doi.org/10.1111/j.1540-8167.2008.01326.x>
98
- 99 Haïssaguerre, M., Derval, N., Sacher, F., Jesel, L., Deisenhofer, I., de Roy, L., Pasquié, J.-L., Nogami, A., Babuty, D., Yli-
100 Mayry, S., De Chillou, C., Scanu, P., Mabo, P., Matsuo, S., Probst, V., Le Scouarnec, S., Defaye, P., Schlaepfer, J.,
101 Rostock, T., ... Clémenty, J. (2008). Sudden cardiac arrest associated with early repolarization. *The New England Journal*
102 *of Medicine*, 358(19), 2016–2023. <https://doi.org/10.1056/NEJMoa071968>
103
- 104 Hu, D., Barajas-Martínez, H., Pfeiffer, R., Dezi, F., Pfeiffer, J., Buch, T., Betzenhauser, M. J., Belardinelli, L., Kählig, K.
105 M., Rajamani, S., DeAntonio, H. J., Myerburg, R. J., Ito, H., Deshmukh, P., Marieb, M., Nam, G.-B., Bhatia, A., Hasdemir,

- 106 C., Haïssaguerre, M., ... Antzelevitch, C. (2014). Mutations in SCN10A are responsible for a large fraction of cases of
107 Brugada syndrome. *Journal of the American College of Cardiology*, 64(1), 66–79.
108 <https://doi.org/10.1016/j.jacc.2014.04.032>
109
- 110 Hu, D., Barajas-Martínez, H., Terzic, A., Park, S., Pfeiffer, R., Burashnikov, E., Wu, Y., Borggrefe, M., Veltmann, C.,
111 Schimpf, R., Cai, J. J., Nam, G.-B., Deshmukh, P., Scheinman, M., Preminger, M., Steinberg, J., López-Izquierdo, A.,
112 Ponce-Balbuena, D., Wolpert, C., ... Antzelevitch, C. (2014). ABCC9 is a novel Brugada and early repolarization syndrome
113 susceptibility gene. *International Journal of Cardiology*, 171(3), 431–442. <https://doi.org/10.1016/j.ijcard.2013.12.084>
114
- 115 Iguchi, K., Noda, T., Kamakura, S., & Shimizu, W. (2013). Beneficial effects of cilostazol in a patient with recurrent
116 ventricular fibrillation associated with early repolarization syndrome. *Heart Rhythm*, 10(4), 604–606.
117 <https://doi.org/10.1016/j.hrthm.2012.11.001>
118
- 119 Koncz, I., Gurabi, Z., Patocskaï, B., Panama, B. K., Szél, T., Hu, D., Barajas-Martínez, H., & Antzelevitch, C. (2014).
120 Mechanisms underlying the development of the electrocardiographic and arrhythmic manifestations of early repolarization
121 syndrome. *Journal of Molecular and Cellular Cardiology*, 68, 20–28. <https://doi.org/10.1016/j.yjmcc.2013.12.012>
122
- 123 Matsui, K., Kiyosue, T., Wang, J. C., Dohi, K., & Arita, M. (1999). Effects of pimobendan on the L-type Ca²⁺ current and
124 developed tension in guinea-pig ventricular myocytes and papillary muscle: Comparison with IBMX, milrinone, and
125 cilostazol. *Cardiovascular Drugs and Therapy*, 13(2), 105–113. <https://doi.org/10.1023/a:1007779908346>
126
- 127 Napolitano, C., & Antzelevitch, C. (2011). Phenotypical manifestations of mutations in the genes encoding subunits of the
128 cardiac voltage-dependent L-type calcium channel. *Circulation Research*, 108(5), 607–618.
129 <https://doi.org/10.1161/CIRCRESAHA.110.224279>
130
- 131 Patocskaï, B., Barajas-Martínez, H., Hu, D., Gurabi, Z., Koncz, I., & Antzelevitch, C. (2016). Cellular and ionic
132 mechanisms underlying the effects of cilostazol, milrinone, and isoproterenol to suppress arrhythmogenesis in an

133 experimental model of early repolarization syndrome. *Heart Rhythm*, 13(6), 1326–1334.

134 <https://doi.org/10.1016/j.hrthm.2016.01.024>

135

136 Shinohara, T., Ebata, Y., Ayabe, R., Fukui, A., Okada, N., Yufu, K., Nakagawa, M., & Takahashi, N. (2014). Combination

137 therapy of cilostazol and bepridil suppresses recurrent ventricular fibrillation related to J-wave syndromes. *Heart Rhythm*,

138 11(8), 1441–1445. <https://doi.org/10.1016/j.hrthm.2014.05.001>

139

140 Varró, A., & Lathrop, D. A. (1990). Sotalol and mexiletine: Combination of rate-dependent electrophysiological effects.

141 *Journal of Cardiovascular Pharmacology*, 16(4), 557–567. <https://doi.org/10.1097/00005344-199010000-00006>

142

143 Watanabe, H., Nogami, A., Ohkubo, K., Kawata, H., Hayashi, Y., Ishikawa, T., Makiyama, T., Nagao, S., Yagihara, N.,

144 Takehara, N., Kawamura, Y., Sato, A., Okamura, K., Hosaka, Y., Sato, M., Fukae, S., Chinushi, M., Oda, H., Okabe, M., ...

145 Makita, N. (2011). Electrocardiographic characteristics and SCN5A mutations in idiopathic ventricular fibrillation

146 associated with early repolarization. *Circulation. Arrhythmia and Electrophysiology*, 4(6), 874–881.

147 <https://doi.org/10.1161/CIRCEP.111.963983>

148

149 **Appendix figure legend**

150 **Figure A1.** Representative action potential traces from canine Purkinje fibers showing the effects of
151 10 μM cilostazol (continuous lines) in the following models of the early repolarization syndrome (ERS,
152 dotted lines): pinacidil 5 μM + acetylcholine 5 μM (Model 1; A), NS5806 7 μM + pinacidil 5 μM +
153 acetylcholine 5 μM (Model 2; B), mexiletine 20 μM + NS5806 7 μM (Model 3; C), and nisoldipine
154 1 μM + NS5806 7 μM + acetylcholine 5 μM (Model 4; D).

Draft

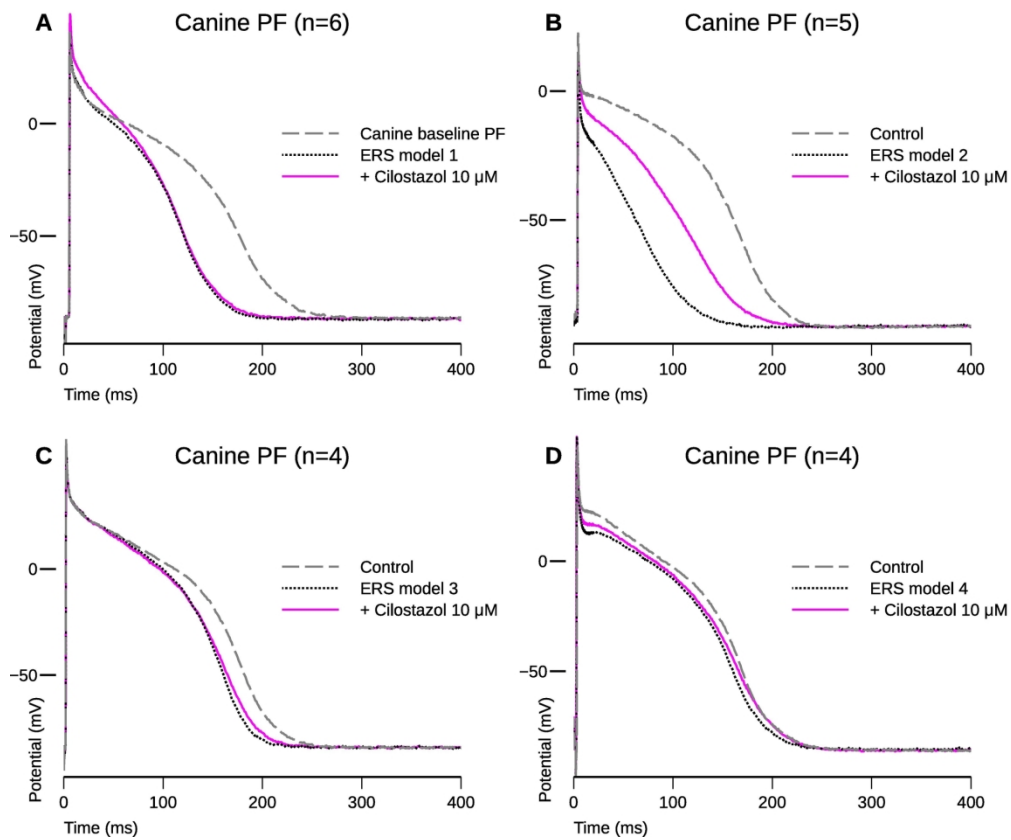


Figure A1. Representative action potential traces from canine Purkinje fibers showing the effects of 10 μ M cilostazol (continuous lines) in the following models of the early repolarization syndrome (ERS, dotted lines): pinacidil 5 μ M + acetylcholine 5 μ M (Model 1; A), NS5806 7 μ M + pinacidil 5 μ M + acetylcholine 5 μ M (Model 2; B), mexiletine 20 μ M + NS5806 7 μ M (Model 3; C), and nisoldipine 1 μ M + NS5806 7 μ M + acetylcholine 5 μ M (Model 4; D).

177x149mm (300 x 300 DPI)